Investigation of Mg2+ ion on Structural, Morphological, FTIR, Dielectric and AC Conductivity of PVDF-HFP Based Solid Polymer Electrolytes and Application to Electrochemical Cell

Anna Mallikarjun
Department of Physics
Sangeetha Mahendrakar
Guru Nanak Institutions Technical Campus
M Vikranth Reddy
Department of Physics
M Jaipal Reddy (mjaipalreddy@gmail.com)
Department of Physics
J Siva Kumar
Department of Physics
T Sreekanth
Department of Physics

Research Article

Keywords: Poly (vinylidene-fluoride-hexafluoroproplyene), SEM, XRD, FTIR, DC ionic conductivity, Mg(ClO4)2 , solution casting technique

Posted Date: May 28th, 2021

DOI: https://doi.org/10.21203/rs.3.rs-560131/v1

Investigation of Mg^{2+} ion on Structural, Morphological, FTIR, Dielectric and AC Conductivity of PVDF-HFP Based Solid Polymer Electrolytes and Application to Electrochemical Cell

A Mallikarjun[1,2], M Sangeetha[3], M Vikranth Reddy[4], M Jaipal Reddy[5*], J Siva Kumar[6*], T Sreekanth[7]

[1] Department of Physics, JNTUH, Kukatpally, Hyderabad, Telangana, India
[1,2] mallikarjun.a@saimail.com
[2] Department of Physics, Vignan's Institute Of Management And Technology For Women, Hyderabad, Telangana, India
[1,2] mallikarjun.a@saimail.com
[3]Department of Humanities and Science, Guru Nanak Institutions Technical Campus, Ibrahimpatnam, Hyderabad, India
[3]radiocurie99@gmail.com
[4]Nilima Organics Private Ltd., Plot No. 105 & 106, IDA Uppal, Hyderabad, India
[4]vikranth997@gmail.com
[5]Department of Physics, Palamur University, Mahabubnagar, Telangana, India
[7]mjaipalreddy@gmail.com
[6]Department of Physics, Osmania University, Hyderabad, Telangana, India
[8]j siva k@yahoo.co.in
[6]Department of Physics, JNTUH College of Engineering Jagtial, Telangana India.
[9]srikanth2t@gmail.com

Abstract

In this paper, solid polymer electrolytes comprising of Poly (vinylidene-fluoride-hexafluoropropylene) (PVDF-HFP) polymer and Mg $(ClO_4)_2$ salt were prepared by employing the solution casting technique. The fabricated polymer-salt electrolyte membranes are exposed to XRD, FTIR and SEM studies. The real and imaginary part of dielectric permittivity is illustrated with the Cole-Cole plot. Static dielectric constant (ε_s), dynamic dielectric constant (ε_∞), dielectric strength ($\Delta\varepsilon$), dielectric loss (tanδ) and relaxation time (τ) are determined using the Cole-Cole plot. The electrochemical properties; cell stability, cell discharge characteristics, dc and ac

conductivity are analyzed. Structural studies of XRD peaks are broadened to confirm the amorphous phase of polymer matrix. Morphological studies shows the presence of interlinked micro-pores promote for ease of mobility of Mg^{2+} ions which attribute to enhance ionic conductivity. The static dielectric constant (ε_s), dynamic dielectric constant (ε_∞), dielectric strength ($\Delta\varepsilon$), dielectric loss (tanδ) reach maximum but relaxation time (τ) decreases for an optimal concentration ratio of (100:40) PVDF-HFP: Mg $(ClO_4)_2$ that reveals fast hopping of ions from one site of the polymer chain to another. The highest ionic conductivity of 7.73333x 10^{-4} Scm^{-1} is obtained at room temperature for [PVDF-HFP: $Mg(ClO_4)_2$] polymer-salt electrolyte. The cell discharge characteristics of OCV and SCC of Mg/ [PVDF-HFP: $Mg(ClO_4)_2$] /I+C cell are found to be 1.8 V and 120 mA respectively The electrochemical stability was observed with a constant voltage of 0.43volt in a positive cycle and 0.4 volts of negative potential which favors an electrochemical membrane for battery applications

Key words: Poly (vinylidene-fluoride-hexafluoroproplyene), SEM, XRD, FTIR, DC ionic conductivity, $Mg(ClO_4)_2$, solution casting technique.

1. Introduction

Solid-state electrochemical cells have high demand at present in modern technology. It has been developed by modifying the polymer electrolytes to enhance conductivity and stability at ambient temperature for potential applications and in energy storage devices. In the process of developing good ionic conductive polymer electrolytes, plasticizers are used which are made of complex polymer electrolyte like PEO/PC/EC/lithium, PAN–PC/EC–$LiClO_4$, PAN–PC/EC–$LiCF_3SO_3$, PAN–

PC/EC–$LiAsF_6$, and PMMA–PC/EC–$LiAsF_6$ [1 - 4]. These complex composite solid polymer electrolytes have potential advantages over conventional solid polymer electrolytes as they exhibit better mechanical strength, higher ionic conductivity, and better temperature stability. Major research work is carried out with various lithium salts LiX ($X = I, Cl, Br, ClO_4, CF_3SO_3, BF_4, AsF_6, PF_6$ etc) of low lattice energies dissolved in high molecular weight solid polymer electrolytes. Despite Li-ion salt complex composite structured polymer electrolytes, the magnesium-based salts are used, and prepared to attain good mechanical strength, temperature stability, and high ionic conductivity. Mg^{2+} ion-based polymer electrolytes are of low cost, easy to handle, and have a divalent cationic conductivity mechanism. Therefore $Mg(ClO_4)_2$ salt is incorporated in PVDF-HFP polymer to fabricate Mg-based solid polymer electrolyte membranes [5].

Besides, magnesium-based batteries are safe and reliable for electric vehicles and domestic applications. The battery performance of magnesium ion electrolytes is very close to lithium ion but avoids explosive hazards that occur in lithium ion batteries [5, 6]. The Li- ion is monovalent but the Mg-ion is divalent in nature. Even Mg is a relatively earth-abundant material, cheaper, lightweight and environmentally friendly [7]. Magnesium perchlorate $Mg(ClO_4)_2$ is a fast ion conducting salt and its incorporation in a polymeric system is expected to get fair complexation with the polymer due to its large anions. Mg^{2+}ion decoupling from the segmental motion of polymer chain is occurring due to large ionic aggregates [8 - 10]. The improvised maximum ionic conductivity is found to be of magnitude 10^{-5} S cm^{-1} at room temperature. The increased conductivity depends on ion migration through

interlinked network of pores which is an important factor for ionic mobility. It has been observed that the critical moisture effect of $Mg(ClO_4)_2$ is very less when compared with various lithium salts. Magnesium batteries may turn up as an alternate for the next rank batteries due to the intrinsic advantage of the Mg metal. Owing to the divalent property of Mg^{2+}, this battery can provide a higher theoretical volumetric capacity (3832 $mAh{\cdot}cm^{-3}$) than Li (2062 $mAh{\cdot}cm^{-3}$). So, Mg batteries are spirited for energy storage devices [10,11]. The Mg^{2+} ionic radius is near to Li ionic radius [12]. Hence, $Mg(ClO_4)_2$ is incorporated in PVDF-HFP polymer which has enough amorphous nature with a large number of interlinked micro-pores and, results are reported in this paper. Based on this polymer electrolyte an electrochemical cell has been fabricated and their battery discharge characteristic is studied.

2. Experimental

Polymer PVDF-HFP from Sigma Aldrich with average molecular weight $4x10^5$ and magnesium perchlorate $Mg(ClO_4)_2$ from Sigma Aldrich are used to prepare the polymer electrolytes. Different concentrations of PVDF-HFP and $Mg(ClO_4)_2$ are separately added to THF solvent at room temperature and stirred continuously with a magnetic stirrer for 10 hours to obtain clear solutions. Then both the solutions were mixed and stirred continuously for 4 hours to get a homogeneous solution. Finally, the solution is poured into polypropylene Petri dishes and allowed to dry at 60 ^{0}C in a vacuum oven for the evaporation of the solvent. This yields a stable free-standing film of thickness ~ 150μm. These films are stored in vacuum desiccators and subjected to various characterization techniques. A picture of the

prepared [PVDF-HFP: $Mg(ClO_4)_2$] polymer-salt electrolyte Membrane is illustrated in Fig. 1.

Fig.1 Illustrates a picture of prepared (PVDF-HFP: Mg $(ClO_4)_2$) polymer-salt electrolyte Membrane.

XRD patterns of [PVDF-HFP: $Mg(ClO_4)_2$] polymer membranes are recorded with Philips X' pert Pro diffractometer, where X-rays of wavelength 1.5406 A^o generated by a Cu-K_α source. The diffraction patterns are recorded at an angle 2θ from $10^o$to 80^o. The polymer electrolytes are subjected to spectroscopic FTIR study using the BRUCKER spectrophotometer in the wavenumber range from 400 to 4500 cm^{-1} at a scan of 1 cm^{-1}. To investigate the surface structure of these films Scanning Electron Microscopy (SEM) micrographs were recorded using the Carl Zeiss SEM. DC conductivity studies are obtained in the temperature range from 303K to 383 K with the aid of the Keithley meter. Using this electrolyte membrane an electrochemical cell has been fabricated in the configuration Mg / (PVDF-HFP: $Mg(ClO_4)_2$ / (I_2+C) and the characteristics of cell discharge at an ambient temperature for a constant load of $1K\Omega$ is studied with the Keithley meter and electrochemical stability of cyclic voltammetry are analyzed with Gamry 5000

Interface potentiostat. And the Electrical impedance spectroscopic studies (EIS) are characterized with E4980A Precision LCR Meter.

3. Results and discussion

3.1 XRD analysis

XRD spectral data of (PVDF-HFP: Mg $(ClO_4)_2$) electrolyte membranes are used to study the crystalline/ amorphous nature of the polymer-salt electrolyte. Fig. 2 shows the XRD patterns with Bragg's angle 2θ versus relative intensity at room temperature for pure PVDF-HFP and various concentration ratios of [PVDF-HFP: $Mg(ClO_4)_2$] polymer electrolyte films. The XRD peaks of pure PVDF-HFP polymer are broad as shown in Fig. 2(a) and appear at 20.3°, 27° and 38°. This illustrates the semicrystalline nature of PVDF-HFP polymer. The Mg $(ClO_4)_2$ salt shows high intense peaks at angle 2θ=10°, 21.55°, 22.94°, 27°, 39°, and 40° which represents the crystalline nature of ionic salt [13]. Various concentrations of Mg $(ClO_4)_2$ are incorporated in PVDF-HFP and it is observed remarkable variation in PVDF-HFP: Mg $(ClO_4)_2$ polymer-salt electrolyte films. From Fig. 2 (b) – (e), it is clear that on the addition of various concentrations of Mg $(ClO_4)_2$ salt to PVDF-HFP, the intensity of XRD spectral peaks of PVDF-HFP polymer are gradually reduced, broadened and shifted from 20.3^0 and 38.67^0 to 23.7^0 and 41.27^0 respectively, and the characteristic peak of PVDF-HFP at 27° has completely vanished. This confirms the gradual change from the semi-crystalline phase to the amorphous nature of the PVDF-HFP. Moreover, the best amorphous nature is noticed at an optimum concentration ratio of (100:40) of PVDF-HFP: $Mg(ClO_4)_2$ polymer-salt electrolyte as depicted in Fig. 2(e).

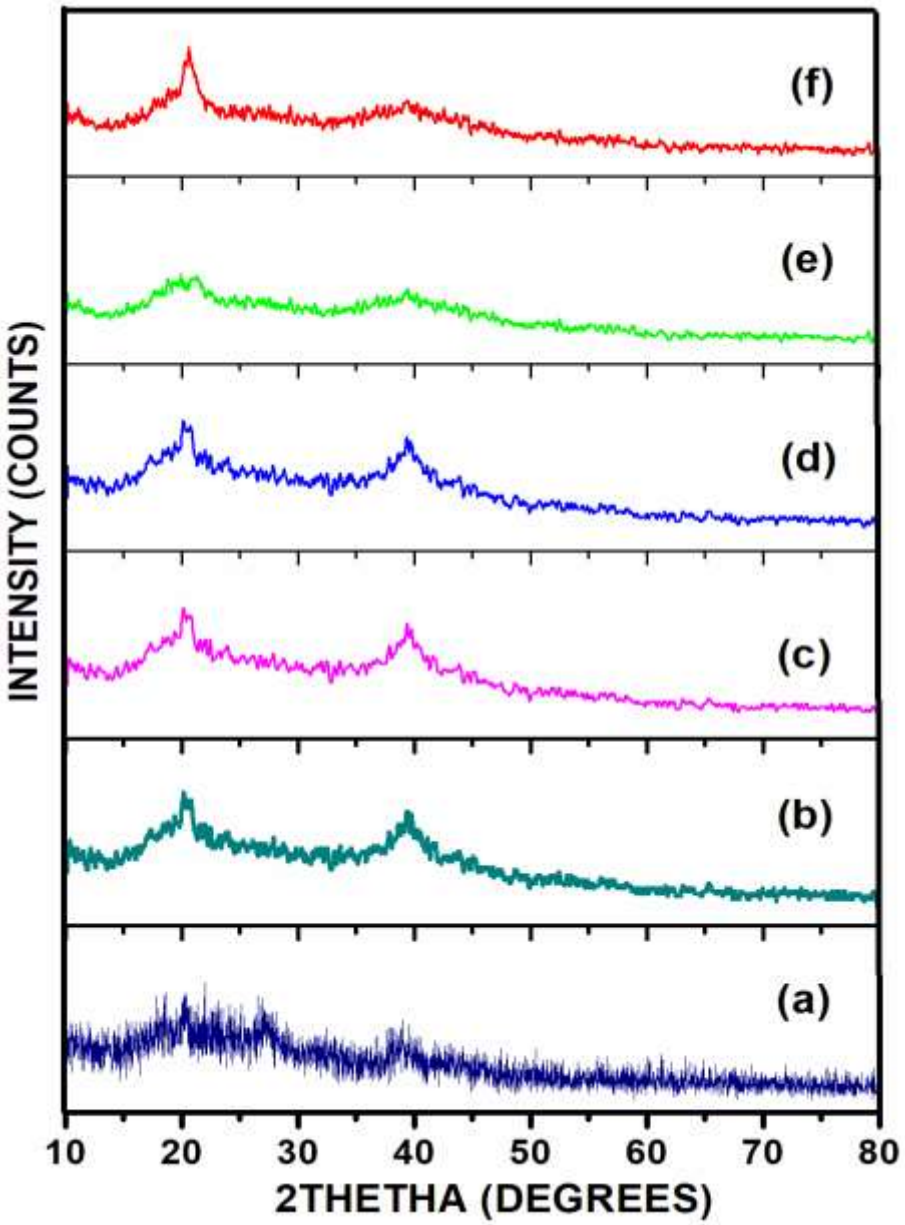

Fig. 2 Illustrates XRD spectrum of PVDF-HFP polymer with different concentrations of $Mg(ClO_4)_2$ salt (a) 0% (b) 10% (c) 20% (d) 30% (e) 40% and (f) 50%

It is obvious that $Mg(ClO_4)_2$ interaction with host polymer PVDF-HFP matrix leads to a decrease of intermolecular interaction among the polymer chain which in turn reduces the crystalline phase and hence improves the amorphous

region [13]. Thus XRD graph suggests an increase in the amorphous phase at an optimum concentration of polymer-salt electrolyte ratio. Further increase in the concentration of $Mg(ClO_4)_2$, the intensity of XRD peak is slightly increased representing again acquiring the semi-crystalline nature of the PVDF-HFP polymer as clearly observed in Fig. 2(f). Similar results are obtained for PVDF-HFP with different salts due to interaction as discussed by the researchers [13, 14].

3.2 FTIR analysis

FTIR analysis is a significant tool to investigate the presence of functional groups and blending of salt $Mg(ClO_4)_2$ in PVDF-HFP host polymer. The interaction of Mg^{2+}ion with the PVDF-HFP electrolyte system induces changes in the vibrational frequencies of the polymer-salt matrix. The recorded FTIR spectra of pure PVDF-HFP and dopant with different concentrations of Mg $(ClO_4)_2$ are shown in Fig. 3. In the FTIR absorption spectrum of PVDF-HFP the vibration bands assigned at 790, and 1062 cm^{-1} peaks corresponds to α phase crystalline nature, and vibration bands at 842 cm^{-1} indicate β and γ phase respectively [15 - 17]. Both α and β phases are two types of crystalline phases of PVDF units [13, 18 –20] while the γ phase represents an amorphous phase of HFP units of PVDF-HFP [18, 21]. The low transmittance peaks at 844 cm^{-1} and 1286 cm^{-1}, assigned to the long trans-sequence of ferroelectric β-phase of PVDF-HFP are absolved due to the effect of Mg^{2+} ion interaction with PVDF-HFP polymer [22 - 24]. Moreover the intensity peak of PVDF-HFP at 1286 cm^{-1} decreases and shifts to 1352 cm^{-1} due to the effect of Mg^{2+} ion on the bond length of host polymer chains.

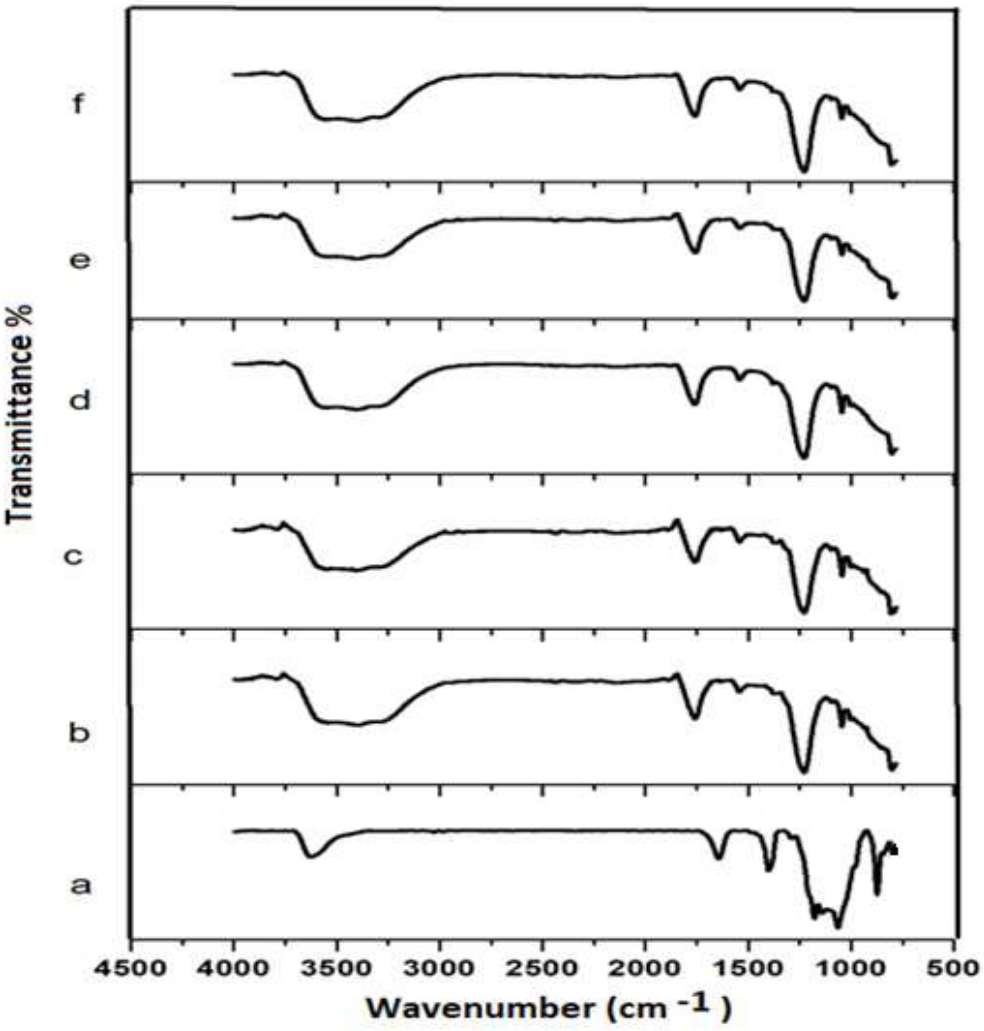

Fig. 3 FTIR spectrum of PVDF-HFP polymer blend with different concentrations of $Mg(ClO_4)_2$ salt (a) 0% (b) 10% (c) 20% (d) 30% (e) 40% and (f) 50%

The absorption peak of PVDF-HFP at 804 cm^{-1} predicts -C-F- wagging and the disappearance of this peak provides evidence of interaction of $Mg^{2+}$with the polymer host. The peak assigned at 798 cm^{-1}corresponds to skeleton deformation which is found to be reduced due to the complexation of polymer salt indicating a phase transition from crystalline to amorphous phase. The vibration peak of PVDF-

HFP polymer assigned at 871cm^{-1}corresponds to CH_2 rocking has disappeared and a new vibrational band appeared at 1041 cm^{-1} represents the amorphous phase [25]. The bending of C-C- band is observed at 1070 cm^{-1} and the peak at 1400 cm^{-1} corresponds to the vibrational frequency of CH_2 which deforms and the intensity of the peak gradually decreases with the incorporation of Mg $(ClO_4)_2$ salt with PVDF-HFP [25-27]. Another important peak is observed at 1280 cm^{-1} which represents symmetrical stretching of CF. The vibrational band at 1643 cm^{-1} of PVDF-HFP is shifted to 1761 cm^{-1} with an increase in the concentration of $Mg(ClO_4)_2$ ionic salt that attributes to a vibrational mode of $Mg(ClO_4)_2$ [28]. The peaks assigned at 1141cm^{-1} and 1176cm^{-1} correspond to the symmetrical stretching mode of CF_3 and CF_2 groups respectively which shift and merge to appear as a new peak at 1230 cm^{-1}. The scissoring vibration of vinylidene $–CH_2$-CF_2- is observed at 1404 cm^{-1} [29, 30]. The vibrational band of 1402 cm^{-1}disappeared and a new peak was noticed at 1545 cm^{-1} which corresponds to CH_2 deformation [29-31]. The IR bands at 2986 and 3024 cm^{-1} are assigned to symmetric stretching of CH_2 and CH_3, symmetric and asymmetric stretching of C-H. A similar result is also obtained due to the effect of cat-ion interaction with PVDF-HFP when ionic salts are added to PVDF-HFP [31 - 32]. Overall, the intensity of peaks in the region 2986 and 3024 cm^{-1} decreases and disappears with the incorporation of Mg $(ClO_4)_2$ salts [33]. The absorption peak assigned at 3626 cm^{-1} shifts to 3240 cm^{-1} corresponds to the backbone of PVDF-HFP which is affected by the interlinked Mg^{2+} ion with vinylidene $–CH_2$-CF_2-. The anion ClO_4^- interacts with C-H symmetrical stretching mode makes the peak shift from 3626 cm^{-1} to 3240 cm^{-1} [34]. The vibrational bands assigned from 783 cm^{-1} to

812 cm^{-1} correspond to pure PVDF. It is predicted that interaction of Mg^{2+} ion on HFP results in stretching of PVDF interlinked bond to an optimum value which aids to the transition of crystalline phase to amorphous nature. The shift of vibrational bands from 783 - 812 cm^{-1} to 812 - 925 cm^{-1} with decreased intensity confirms the amorphous phase of PVDF-HFP when complexed with Mg $(ClO_4)_2$ salt. The observed vibrational frequencies of the pure PVDF-HFP have been shifted, some bands disappeared and new peaks appeared with the addition of Mg $(ClO_4)_2$, which indicates that the Mg^{2+} ion affects the vibrational mode of PVDF-HFP and suggest the complex formation between PVDF-HFP and Mg $(ClO_4)_2$.

3.3 SEM analysis

SEM micrographs of Fig. 4(a) – (h) illustrate surface morphology of PVDF-HFP and PVDF-HFP with different concentrations of $Mg(ClO_4)_2$ prepared polymer electrolytes. It is perceived that with an increase in the concentration of $Mg(ClO_4)_2$ salt to PVDF-HFP enormous number of fine pores are formed and the size of pores in the polymer-salt matrix is modified and enlarged which aids for ease mobility of ions. It is observed that HFP groups had a positive effect on the mechanical property which is an important factor for enough porosity and the amorphous nature of polymer membranes. Fig.4 (a) exhibits a rough, granular surface with few available dark micro pores representing the semi-crystalline nature of PVDF-HFP polymer. It is obvious that with the addition of various concentration of $Mg(ClO_2)_4$ salt, a smooth texture on the surface with a large number of micro-pores which confirms a phase transition from semi-crystalline to amorphous nature [31]. The pores result in microstructure due to evaporation of solvent [35].

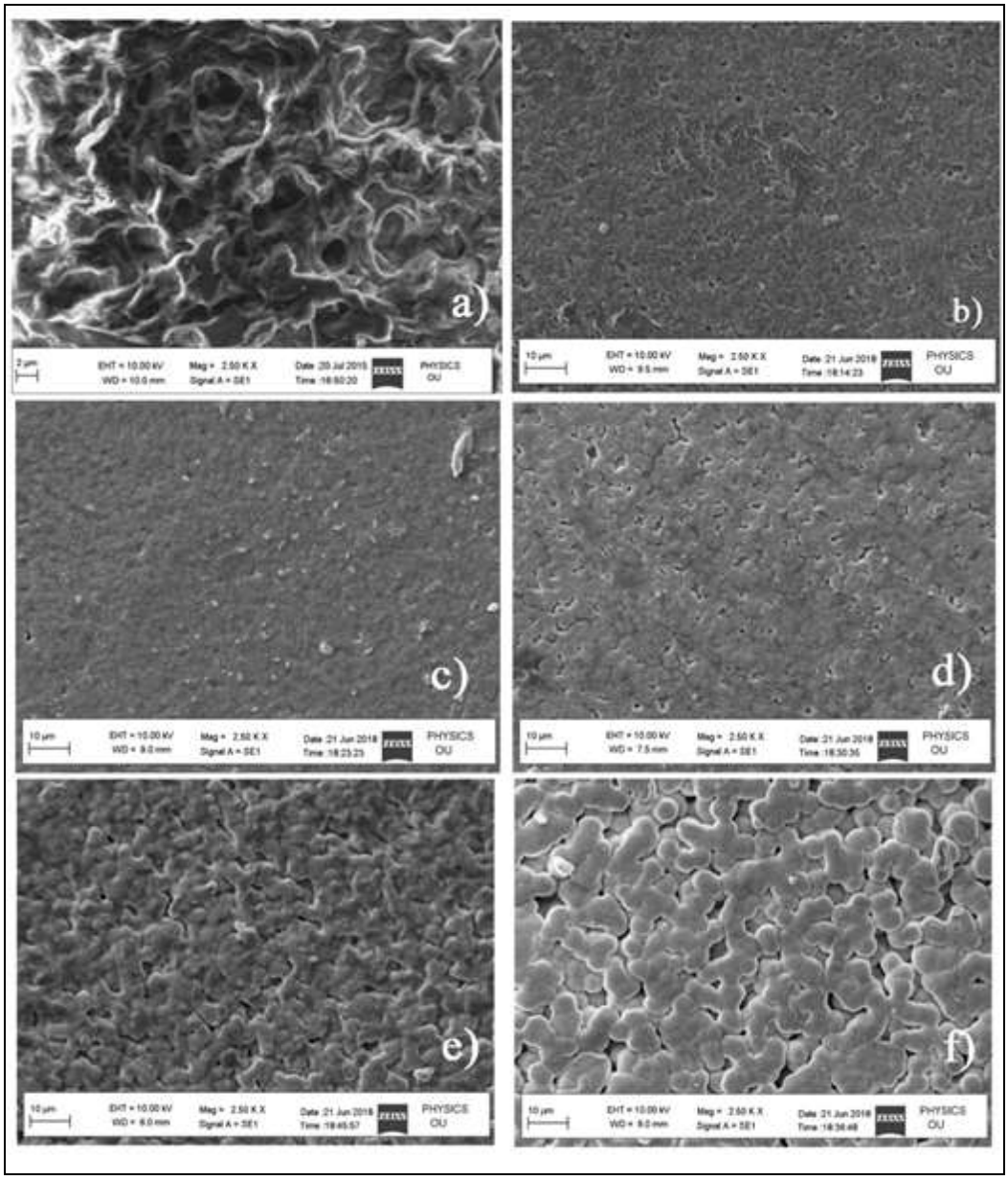

Fig. 4 Illustrates SEM micrographs of of PVDF-HFP polymer with different concentration of Mg $(ClO_4)_2$ salt (a) 0% (b) 10% (c) 20% (d) 30% (e) 40% and (f) 50%

The microporous structure is favorable for the migration of Mg^{2+} ions in polymer texture. The highly porous structure in a polymer matrix is the result of mutual interaction of solvent with polymer to escape from polymer membrane. The interlinked micro-porous polymer matrix promotes the path for migration of Mg^{2+}

ions [36]. The increase in the number of pores and size of pores is responsible for higher absorption of polymer-salt electrolyte and an advantageous factor for ion mobility. The uniform spherical grain size on the surface of SEM images is mainly due to the monomer units of PVDF-HFP. The interaction of Mg^{2+} ions with PVDF-HFP polymer is evidence in the increase of pores size and attaining smooth amorphous phase. It is observed that uniform distribution of interconnected and sufficient size of a large number of micropores with smooth surface appears at an optimum concentration ratio of (100:40) (PVDF-HFP: Mg $(ClO_4)_2$) as shown in Fig. 4(e). This favors amorphous nature and which is also evidenced in XRD analysis.

3.4 DC Conductivity

The DC ionic conductivity of the polymer electrolyte can be calculated using the equation

$$\sigma = \frac{l}{R_b A} \text{S/cm} \qquad (1)$$

Where $l =$ thickness of the polymer sample, $R_b =$ Bulk resistance, A is an area of the sample. The bulk resistance of the sample calculated using $R_b = (V/i)$ where 'V' is voltage and 'i' is current [37]. A graph is plotted between $\ln \sigma$ *and* $\frac{1000}{T} K^{-1}$ for various concentrations of solid polymer electrolytes in the temperature range of 303 to 373 K presented in Fig. 5. The conductivity graph of different concentrations of $Mg(ClO_4)_2$ in PVDF-HFP polymer is presented in Fig. 6.

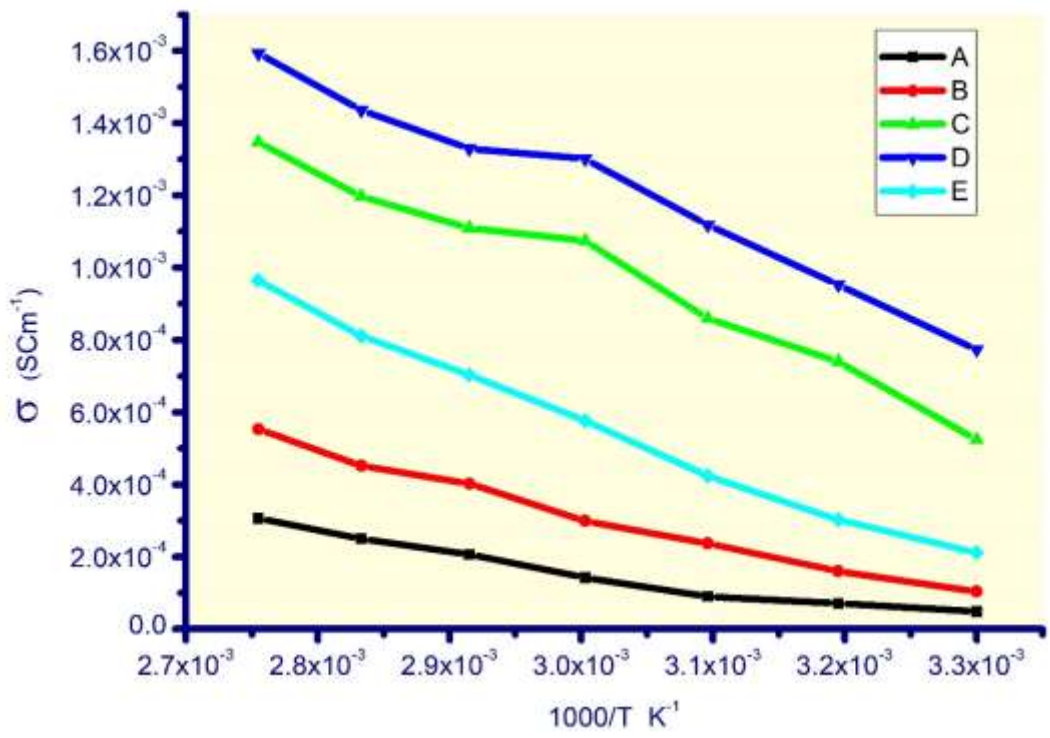

Fig. 5 Temperature dependent DC conductivity of PVDF-HFP with various concentration of Mg $(ClO_4)_2$ polymer-salt electrolytes (A) 10% (B) 20% (C) 30% (D) 40% and (E) 50%

In Fig.5, it is observed that the conductivity increases with a gradual rise of temperature in various concentrations of polymer-salt electrolytes. It is perceived that at a particular optimum concentration of (100: 40) [PVDF-HFP: $Mg(ClO_4)_2$] polymer-salt matrix found maximum conductivity as shown in Fig.5(D) and Fig 6. This shows well compatibility and proper blending of polymer-salt electrolytes. It is clear that at an optimum concentration Mg^{2+} and ClO_4^- ions dissociate freely and generate free charge carriers. Hence, the crystalline phase of the polymer is suppressed, and increased in the amorphous phase is responsible to enhance conductivity which is established in the XRD and SEM results.

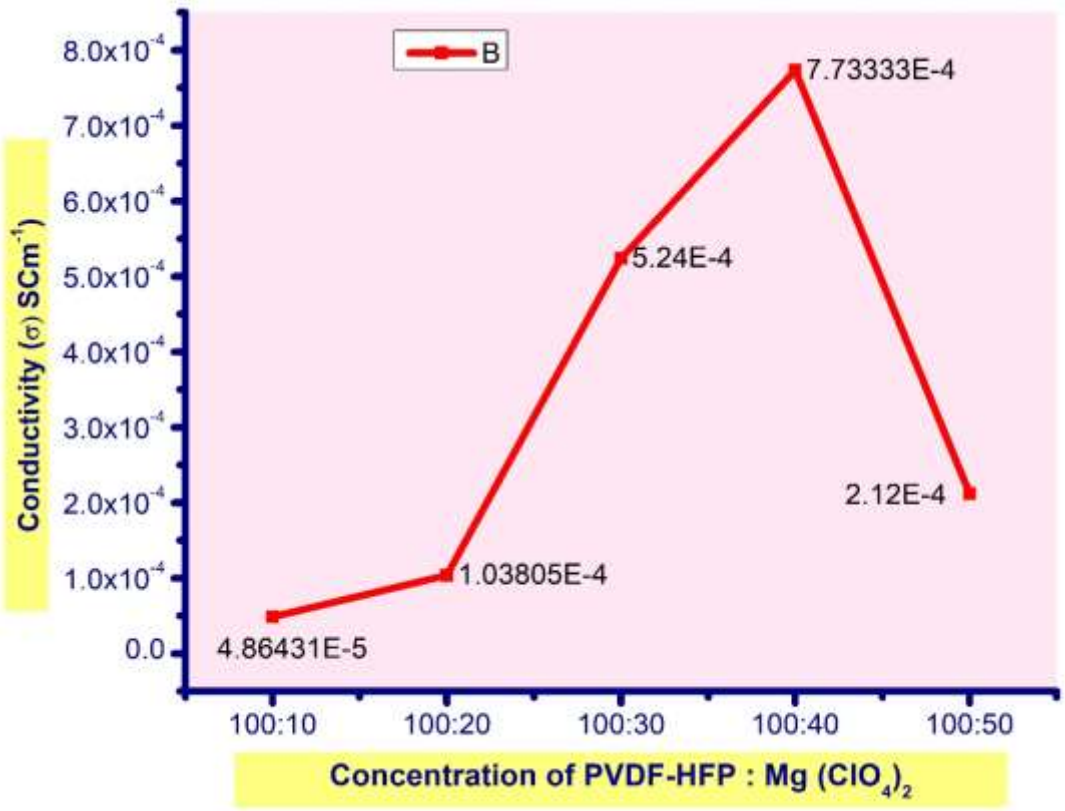

Fig. 6 Variation of DC conductivity for different concentrations of Mg $(ClO_4)_2$ salt in PVDF-HFP polymer

Further, the higher concentration of $Mg(ClO_4)_2$ salt makes ion-pairing Mg^{2+} and ClO_4^- ions, which in turn drop the ionic conductivity of polymer-salt electrolyte as observed in Fig. 5 and Fig. 6. The maximum conductivity of 7.7333 x 10^{-4} S cm^{-1} at 303 K is obtained for (100:40) [PVDF-HFP: Mg $(ClO_4)_2$] polymer-salt electrolyte membrane.

3.5 Structural Model

The XRD, FTIR, and SEM results of PVDF-HFP: $Mg(ClO_4)_2$ polymer-salt electrolytes infer that there is a gradual change from a semi-crystalline phase to an

amorphous phase when $Mg(ClO_4)_2$ salt added to the PVDF-HFP polymer. Fig. 7 presents the Structural Model of PVDF-HFP: $Mg(ClO_4)_2$ Solid Polymer electrolyte. The Mg^{2+} ion interacts with the electronegative nature of the 'F' atom of the host polymer PVDF-HFP matrix, which leads to a decrease of intermolecular interaction among the polymer chain. The intermolecular interaction may reduce the crystalline nature and hence a dominant presence of amorphous phase in PVDF-HFP: $Mg(ClO_4)_2$ polymer-salt electrolytes. The FTIR data also suggested that the interaction of Mg^{2+} ion with the PVDF-HFP polymer; modified the vibrational band positions in the polymer-salt matrix. The found vibrational modes in the pure PVDF-HFP were some shifted, some disappeared and new bands appeared with the addition of Mg $(ClO_4)_2$ salt, hence these changes indicates the Mg^{2+} ion affected the vibrational mode of PVDF-HFP polymer due to interlink between electronegative F atom in PVDF-HFP with Mg^{2+} ion. SEM micrographs have shown a smooth texture on the surface with a large number of micro-pores when Mg salt is added to PVDF-HFP polymer which is evidence of phase change from semi-crystalline to amorphous. The micro-porous structure in polymer-salt electrolyte micrographs is also suggesting that the Mg^{2+} ion interlinked with the electronegative 'F' atom of the host polymer PVDF-HFP and forms a favourable network structure.

The reason for ion transport in this PVDF-HFP: $Mg(ClO_4)_2$ polymer-salt electrolyte system is Mg^{2+} ions hop or may transfer from one site to another in the same polymer chain or to the neighbor polymer chain. Moreover, increase in temperature expands the polymer chains to increase free volume which promotes segmental motion of the polymer chain.

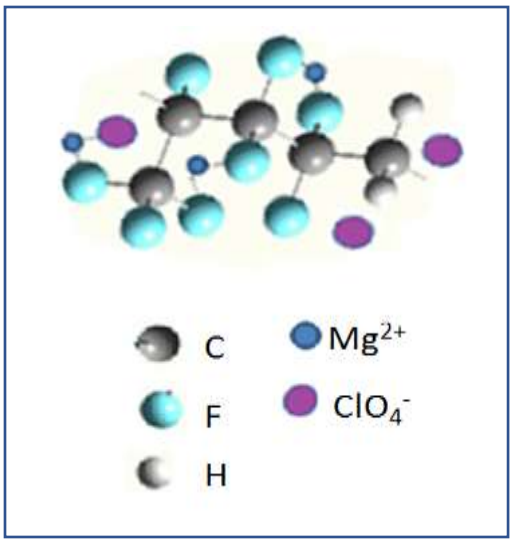

Fig. 7 Structural Model of PVDF-HFP: Mg $(ClO_4)_2$ Solid Polymer electrolyte membrane

3.6 Electrochemical cell characteristics

Electrochemical cell is fabricated with the PVDF-HFP: $Mg(ClO_4)_2$ polymer-salt electrolyte by the configuration of Mg / [100 PVDF – HFP: 40 $Mg(ClO_4)_2$] / (I_2+C).

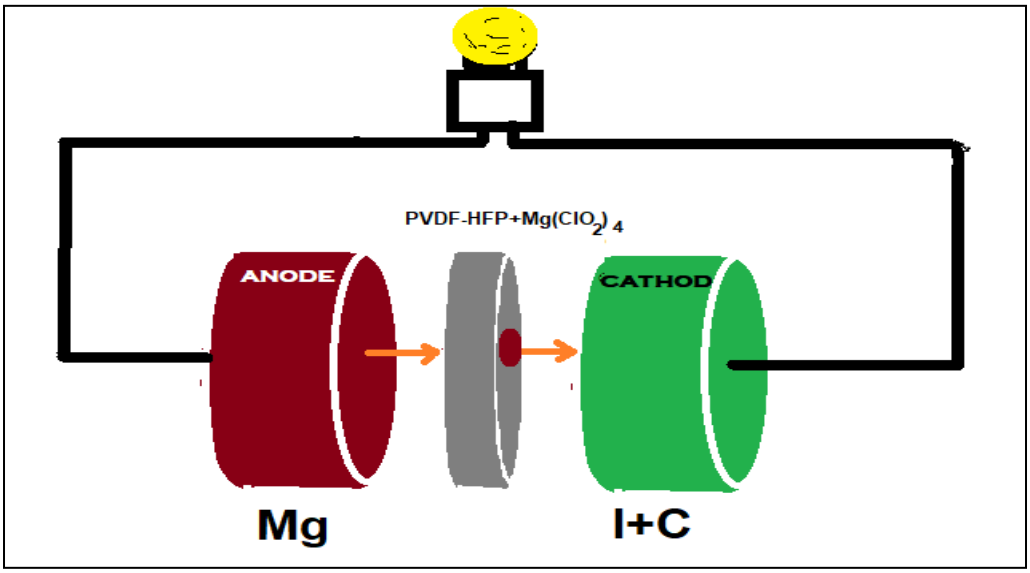

Fig. 8 Mg^{2+} ion electrochemical cell of Mg / [PVDF-HFP: $Mg(ClO_4)_2$] (100:40) / I_2+C for the polymer electrolyte

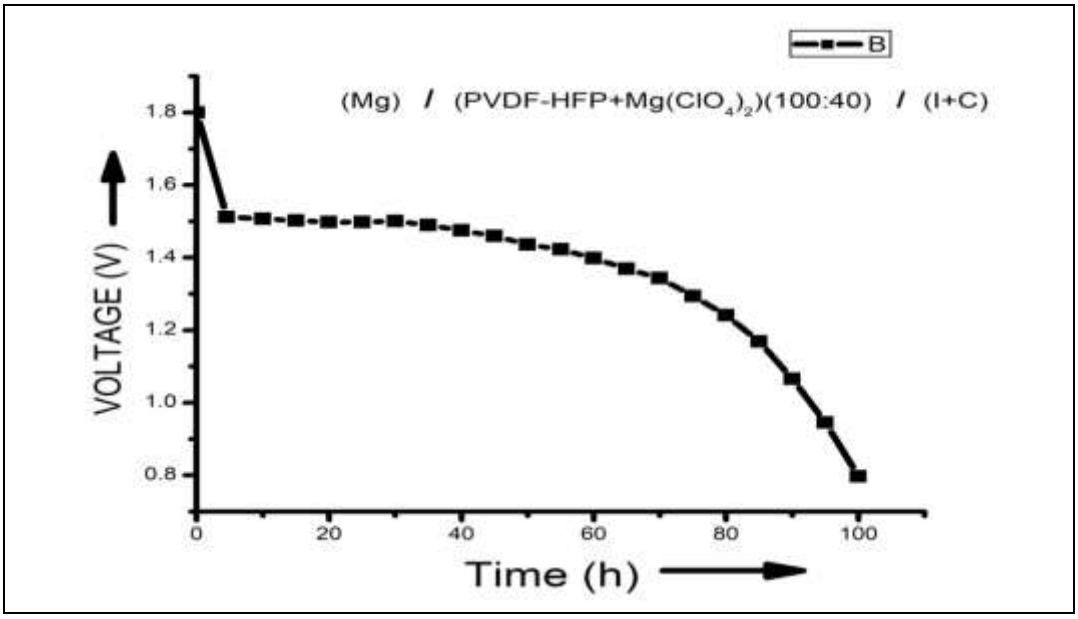

Fig. 9 Voltage Vs Time curve illustrates discharge characteristics of an Electrochemical cell of Mg/100 PVDF-HFP: 40 $Mg(ClO_4)_2$ / I_2 +C

Fig. 8 illustrates the structure configuration of fabricated electrochemical cell Mg / [PVDF-HFP: $Mg(ClO_4)_2$] (100:40) / (I_2+C). Fig. 9 shows the discharge characteristics of the cell at an ambient temperature for a constant load of $1K\Omega$. The open-circuit voltage and short circuit current are measured as 1.8V and120 mA respectively. Open circuited voltage of the cell Mg/PVDF – HFP: $Mg(ClO_4)_2/I_2$+C is dropped to 1.5 V when it is connected to a load of 1KΩ. It is stable for 70 hrs. and a sharp decrease is noticed in the voltage, it may be due to the polarization and formation of a thin layer of salt at the electrode-electrolyte interface [38, 39]. Further work is in progress to improve the cell parameters and capacity.

3.7 Electrochemical stability of polymer electrolyte (Cyclic voltammetry)

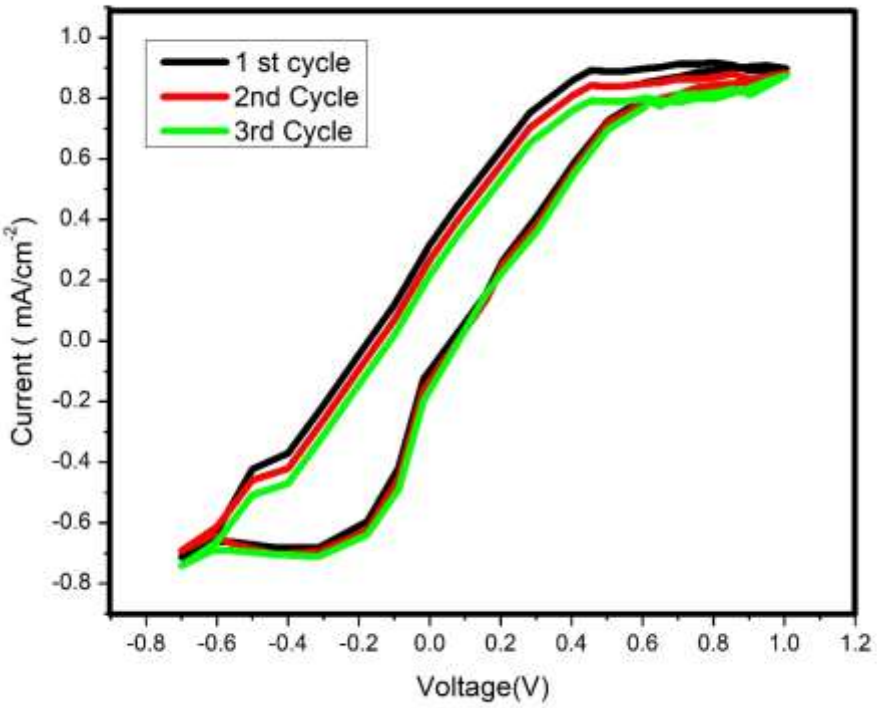

Fig.10 Cyclic voltammetry (CV) curves of PVDF-HFP: Mg $(ClO_4)_2$ polymer electrolyte films at a time interval of 24 hours.

The Stability of the electrochemical cell of PVDF - HFP: Mg $(ClO_4)_2$ was analyzed with the cyclic voltammetry using an "Mg^{+2} / PVDF - HFP: $Mg(ClO_4)_2$ membrane /carbon". The analysis was carried out between -1 V to 1 V at a scan rate of $1mVs^{-1}$ and a temperature of 28^0 C. Here carbon is used as a working electrode and Mg^{2+} metal as unblocking reference or counter electrode. The electrolyte performance studied for the first-day 1st cycle; reveals good performance throughout the cyclic in the electrochemical cell. The same cyclic performance is observed on the 2nd, 3rd, 4th, and 5th day as there is no degradation of an electrochemical cell as

shown in Fig. 10. This result reveals the stability of the electrochemical cell even after 5 days. A fast-rising curve of positive and negative cyclic indicates anode and cathode currents in the cell up to 0.4 V. The electrochemical stability was observed for electrolyte membrane above 0.43 V which reveals the best compatibility of electrochemical membrane for battery applications. The cyclic voltammetry graph reveals that the disassociation of ions, orientation, and migration towards the field gradually increases and attains a uniform saturation state as observed with a constant voltage of 0.43volt in a positive cycle and 0.4 volts of negative potential.

3.8 Dielectric Spectroscopy:

3.8.1 Cole-Cole Plot:

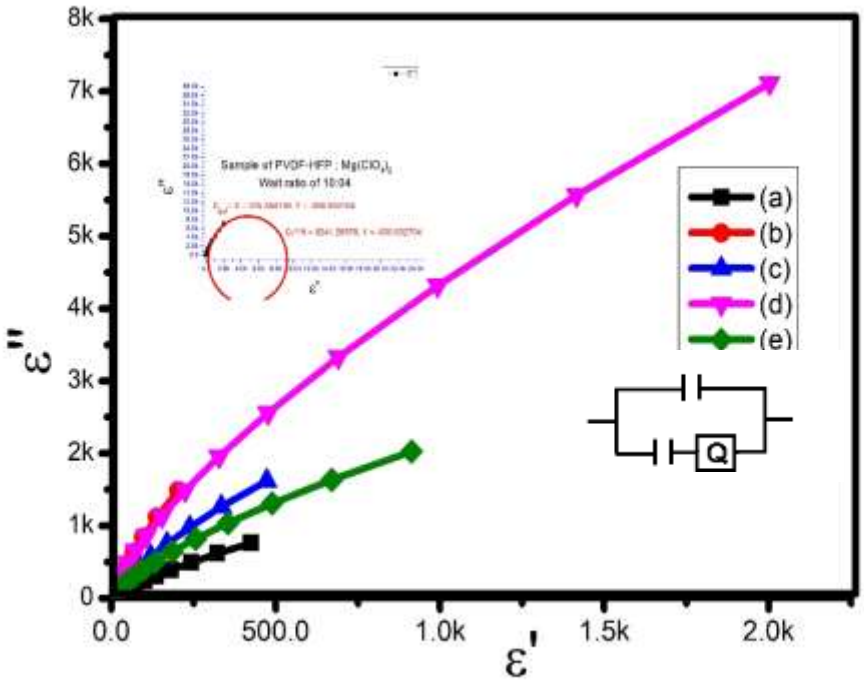

Cole-Cole plot for polymer electrolyte PVDF-HFP: $Mg(ClO_4)_2$

Fig. 11 a) Variation of ε'' imaginary dielectric constant against ε' in the Mg $(ClO_4)_2$ based solid PVDF-HFP polymer electrolyte

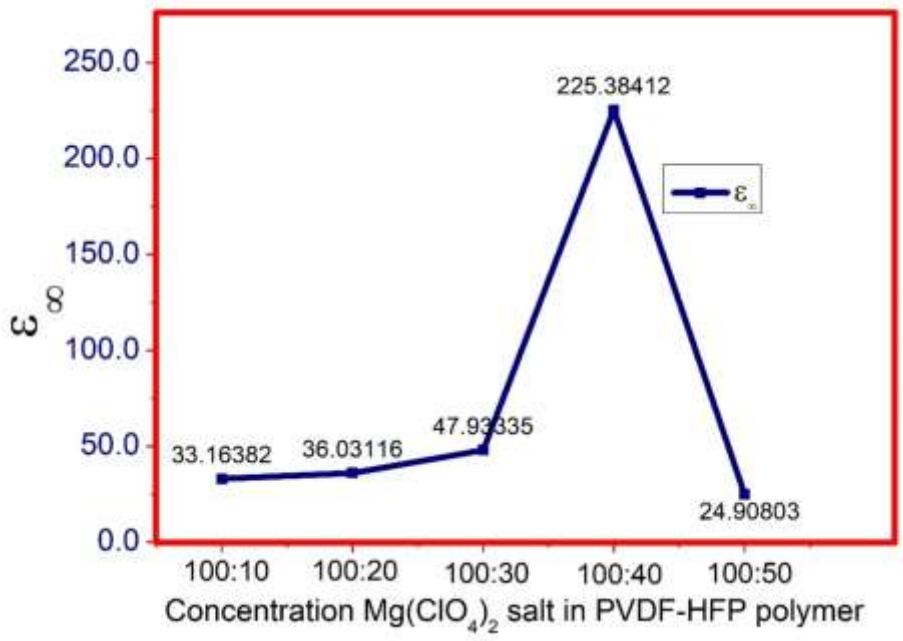

Fig. 11 b) Variation of dynamic dielectric constant (ϵ_∞) with the concentration of Mg $(ClO_4)_2$ salt in the PVDF-HFP polymer electrolyte

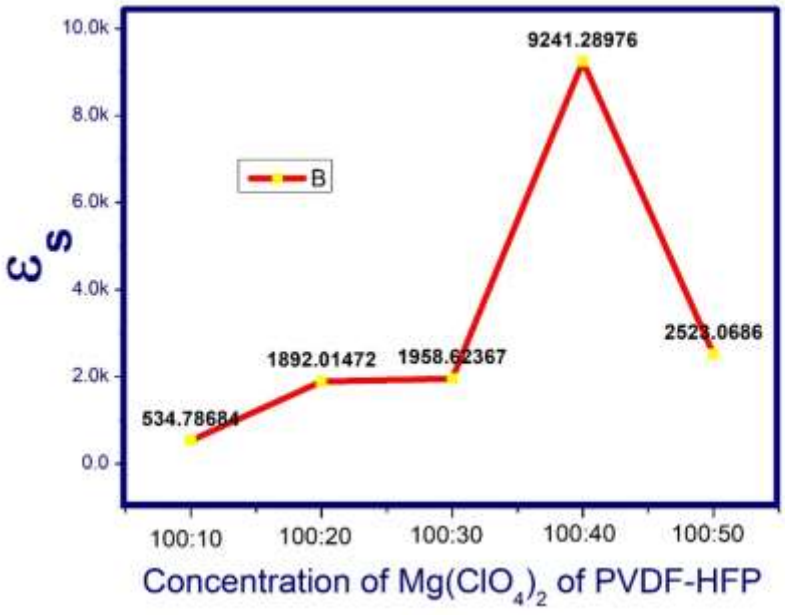

Fig. 11 c) Variation of static dielectric constant with the concentration of Mg $(ClO_4)_2$ salt in the PVDF-HFP polymer electrolyte

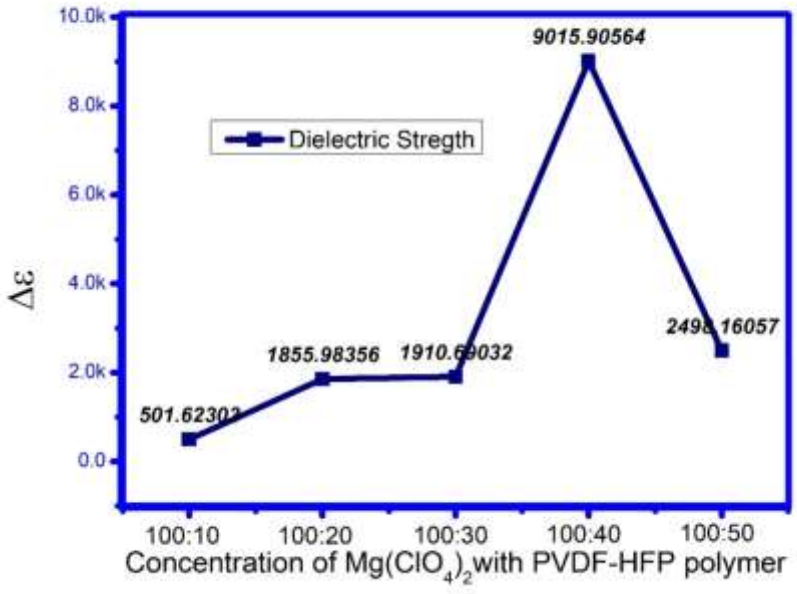

Figure 11 d) Variation of dielectric strength (***Δε***) with the concentration of Mg $(ClO_4)_2$ salt in the PVDF-HFP polymer electrolyte

Cole-Cole plot of the PVDF-HFP based polymer with different concentrations of Mg $(ClO_4)_2$ salt is shown in Fig. 11 a). This reveals the information regarding the relaxation process, inter-operation of dielectric measurements, and also ion segmental motion of the polymer electrolyte with the variation of frequency. The complex dielectric constant ε^* is represented by the combination of real ε' and imaginary part ε'' of a dielectric constant [40, 41, 42]. A plot is drawn between the imaginary part of dielectric permittivity ε'' and a real part of dielectric permittivity ε'; obeys a perfect semicircle of the Debye equation [40, 41, 42]. The semicircle reveals the dielectric behavior at different concentrations of PVDF-HFP: Mg $(ClO_4)_2$ polymer electrolyte as shown in Fig. 11 a). The intersecting point of a semi-circle at the left side axis of the real part of dielectric constant; denotes ε_∞ which is known as dynamic dielectric constant.

$$\varepsilon^* = \varepsilon' - j\varepsilon'' \quad (2)$$

Here ε_s is the static dielectric constant $(x \to 0)$, ε_∞ is the dynamic dielectric constant $(x \to \infty)$, $x = \omega\tau$; ω is the applied angular frequency and τ is the average Debye relaxation time [40, 41, 42].

$$\varepsilon^* = \varepsilon_\infty + \frac{\varepsilon_s - \varepsilon_\infty}{1+jx} \quad (3)$$

$$\varepsilon' = \varepsilon_\infty + \frac{\varepsilon_s - \varepsilon_\infty}{1+x^2} \quad (4)$$

$$\varepsilon'' = \frac{\varepsilon_s - \varepsilon_\infty x}{1+x^2} \quad (5)$$

ε_∞ is also known as high-frequency dielectric constant. The rise in the value of the high-frequency dielectric constant represents the response of ions for the high-frequency electric field as shown in Fig. 11 b). And the right-side intersecting point of a semicircle indicates the static dielectric constant ε_s or low-frequency dielectric constant; which is directly linked with the number of charge carriers at low-frequency. As the concentration of Mg $(ClO_4)_2$ salt is increased in the PVDF-HFP polymer, there is complete disassociation of salt which is evidence of accumulation of charge at the electrodes. This can be understood by the highest value of low-frequency dielectric constant ε_s as noticed in Fig. 11 c). In Fig. 11 a), the semicircle represents the dielectric behavior at different concentrations of PVDF-HFP: Mg $(ClO_4)_2$ polymer electrolyte and the diameter of the circle measures dielectric strength $\Delta\varepsilon = \varepsilon_\infty - \varepsilon_s$ which indicates an increase in the disassociation of salt and a large number of mobility of free ions to the variation of frequency. This results in good ionic conductivity of the polymer electrolyte as clearly represented in Fig. 11

c). It is clear from Fig. 11 b) and Fig. 11 c) that the dynamic and static dielectric constant attain the highest for the optimal concentration the weight ratio of (10:04) (PVDF - HFP: Mg $(ClO_4)_2$) polymer-salt electrolyte. It is noticed that the diameter of the circle becomes large i.e. the dielectric strength $(\Delta\varepsilon = \varepsilon_\infty - \varepsilon_s)$ also increases as it is proportionate to the diameter of a circle (as illustrated in Fig. 11 a) from the concentration ratio of (10:1) to (10:04) in (PVDF - HFP: Mg $(ClO_4)_2$) polymer-salt electrolyte. The reason for this is; an increase in the fast response of ions from the low-frequency electric field to high frequency with an increase in the concentration of salt. Moreover, disassociation of ions and generation of active dipoles enhances the dielectric strength as observed in Fig. 11 d) which is responsible for achieving the highest conductivity and dielectric constant of PVDF-HFP/Mg $(ClO_4)_2$ polymer electrolyte. But further excess addition of salt drops the dielectric strength $(\Delta\varepsilon)$; since the dissociation of salt is reduced due to the accumulation of ionic charges at the electrode and ion to ion interaction increases as clearly noticed in the dielectric strength of Fig. 11 d). This is confirmed with a drop in the diameter of a semi-circle which confirms that a higher concentration of salt more than the optimal value accumulates the ions affects the segmental mobility of ions in the polymer chain. This is the consequence of a low dielectric constant and drops the ionic conductivity of polymer electrolyte for an excess concentration of salt in PVDF-HFP polymer electrolyte.

`3.8.2 Dielectric Loss:

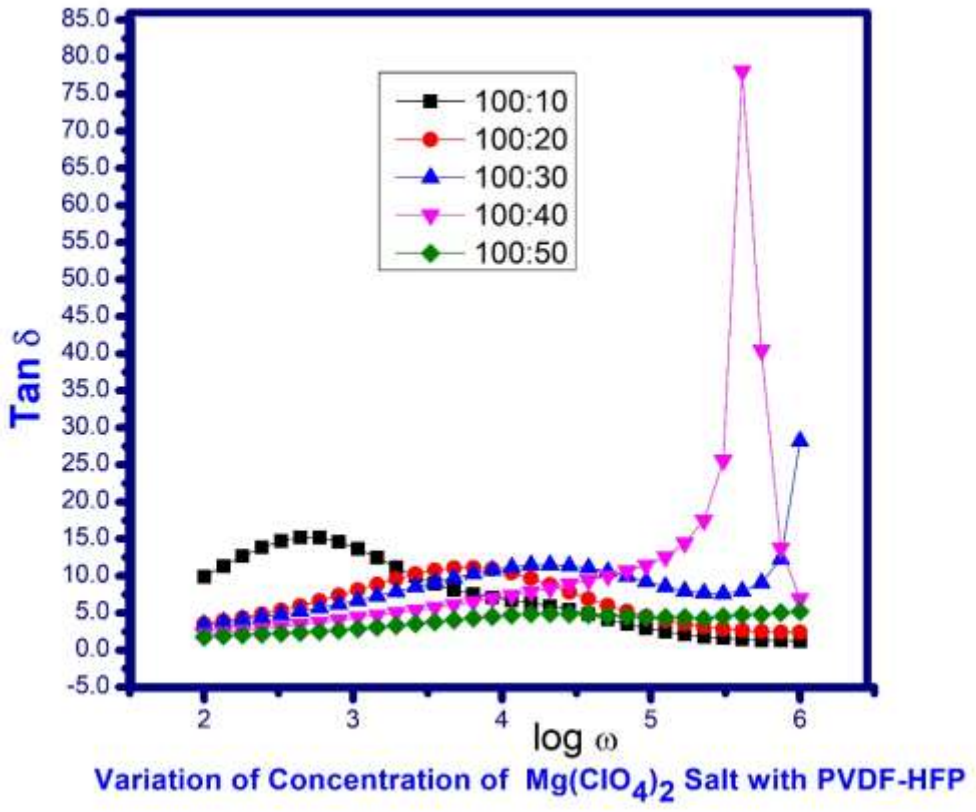

Fig. 12 a) Variation of dielectric loss (Tanδ) against $\log \omega$ of $Mg(ClO_4)_2$ in the PVDF-HFP polymer electrolyte.

It is obvious from Fig. 12 a) that the tangent loss (or a measure of dielectric loss) increases with an increase in the frequency of electric field and attains a maximum peak at an appropriate optimal concentration ratio of (100:400) (PVDF-HFP: $Mg(ClO_4)_2$) polymer electrolyte and it decreases for the higher-frequency. To understand the better effect of the ac electric field on the polymer electrolyte, Fig 12 a) can be divided into three regions. The initial or first region is low-frequency, the

second region is the moderate frequency and the third region called the high frequency. The increase in the domination of the ohmic element is greater than the loss of the capacitive element which can be represented as the low-frequency region. It is observed that there is an increase in the loss of electric energy because more relaxation time (τ) is required for the alignment of ions in the direction of the ac electric field.

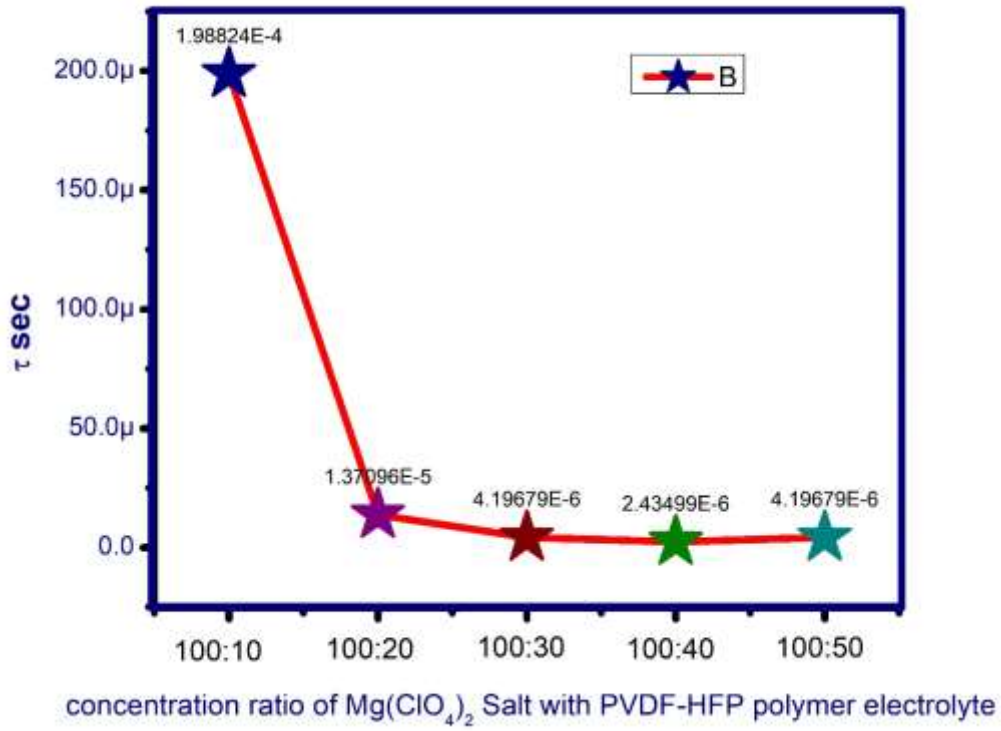

Fig. 12 b) Variation of relaxation time against concentration of $Mg(ClO_4)_2$ salt with PVDF-HFP solid polymer electrolyte**.**

It is observed that a maximum peak is obtained when the frequency of the electric field perfectly matches with the rotational frequency of the polymer molecule and this maximum peak is represented as a moderate-frequency region and energy loss is also high in this region. The maximum energy loss or tangent occurs at

a certain frequency known as the resonance frequency. This may lead to maximum power transfer to the dipoles in the polymer matrix system and hence maximum power loss is releases in the form of heat. The corresponding frequency of high dielectric loss satisfies the equation $\omega\tau = 1$ [40, 43]. The resonance frequency occurs if the frequency of Ohmic and Capacitance components matches with the frequency of the ac electric field that can be noted from Fig. 12 a) and hence the relaxation time is calculated from the maximum peak which is also called as average relaxation time of the polymer electrolyte. But at higher frequencies the capacitance component dominates, hence the domination of the Ohmic element becomes independent of frequency. It is noticed that the relaxation time decreases with the ion orientation in the polymer electrolyte. Moreover, even though the dielectric loss at a higher frequency is less ($tan\delta$), the response of the ions is good to orient and align along the field direction. Hence the polymer electrolyte attains high ionic conductivity and possesses a good dielectric constant. It is perceived that as the $Mg(ClO_4)_2$ salt concentration increases, the relaxation peak shifts from low-frequency to high-frequency owing that the relaxation time decreases which reveals the rapid hopping of Mg ions from one polymer site to another site of the polymer matrix [43, 44]. And a very less relaxation time is obtained for an optimal concentration ratio of (100:40) PVDF-HFP: Mg $(ClO_4)_2$ polymer electrolyte that reveals fast hopping of ions in the polymer matrix from one site of the polymer chain to another as shown in Fig. 12 b). Further, a high tangent loss occurs due to resonance between the applied electric field and more ions in the polymer

electrolyte. Also, a substantial segmental motion of ions attains good ionic conductivity at the higher frequency of the polymer electrolyte.

3.9 The real part of complex AC conductivity

The ac electrical conductivity of the polymer electrolytes is calculated with the equation given below

$$\sigma' = \sigma_{ac} = \omega\varepsilon_0\varepsilon'' = \omega\varepsilon_0\varepsilon' \tan\delta \qquad (6)$$

where ω is the angular frequency, $\boldsymbol{\varepsilon_0}$ is the permittivity of free space, $\varepsilon_0 = 8.854\ x\ 10^{-12}\ F/m$ and $\tan\delta$ = dielectric loss

The complex ac conductivity of the polymer electrolyte can be expressed as

$$\sigma_{ac} = \sigma' + j\sigma'' = \omega\varepsilon_0[\varepsilon'' + j(\varepsilon - \varepsilon_\infty)] \qquad (7)$$

$$\varepsilon^* = \varepsilon' - j\varepsilon'' \qquad (8)$$

$$\varepsilon' = \frac{-z''}{\omega C_0(Z'^2 + Z''^2)} \qquad (9)$$

$$\varepsilon'' = \frac{z'}{\omega C_0(Z'^2 + Z''^2)} \qquad (10)$$

Where ε' and ε'' are the real and imaginary part of the dielectric permittivity respectively, ω is the angular frequency, C_0 is the capacitance of vacuum, $Z'$and Z'' are real and imaginary parts of the electrical impedance [43], which can be measured by an LCR meter. Further, complex conductivity σ_{ac} is the combination of real $\sigma'$and imaginary σ''part of conductivity.

$$\sigma_{ac} = \sigma' + i\sigma'' = \omega\varepsilon_0[\varepsilon'' + j(\varepsilon' - \varepsilon_\infty)] \qquad (11)$$

$$\sigma' = \omega\varepsilon_0\varepsilon'' \qquad (12)$$

$$\sigma'' = \omega\varepsilon_0(\varepsilon' - \varepsilon_\infty) \qquad (13)$$

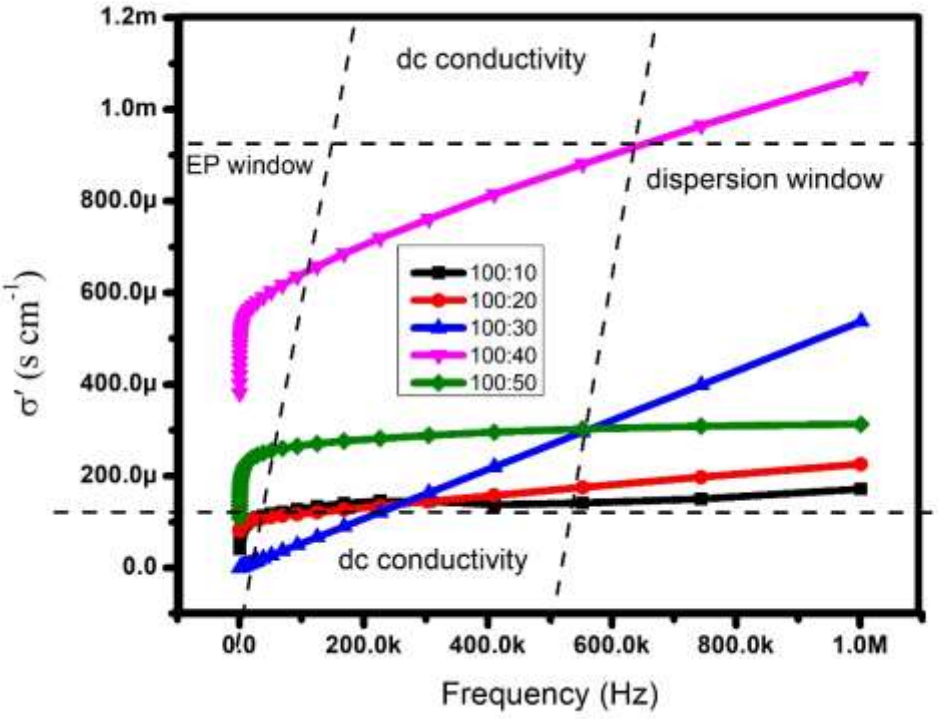

Fig. 13 Variation of real part of conductivity against frequency for different concentration of $Mg(ClO_4)_2$ salt in PVDF-HFP solid polymer electrolyte

The variation of the real part of AC conductivity with the change of frequency is shown in Fig. 13. Three distinct regions are observed in Fig. 13 that depend upon the frequency of an AC electric field. The low-frequency region is the frequency region- I, it is noticed that there is a sharp rise in conductivity occurred due to electrode polarization. This is illustrated as the EP window in Fig. 13. The next followed region is the intermediate region which is also known as the frequency-independent region; here the conductivity does not depend on the frequency, which

reveals the long-range conduction of the charge carriers, and dc ionic transport (hopping) associated with the AC conductivity can be easily understood. In region II there is a gradual increase of ion conductivity for an optimum concentration ratio of (10:04) [PVDF-HFP: Mg $(ClO_4)_2$] polymer electrolyte. It is observed that with an increase in the frequency, more activated ions orient parallel to the ac electric field with less relaxation time. And a small value of the slope represents a linear increase of conductivity with the increase of frequency which represents evidence of activation of new dipoles and hoping of ions from one atomic site to another atomic site. The frequency-dependent electrical conductivity generally obeys Jonscher's power law [45, 46].

$$\sigma(\omega) = \sigma_{dc} + A\omega^n \qquad (14)$$

where $\sigma(\omega)$ denotes the total conductivity, $'\sigma_{dc}'$ is the dc conductivity of the sample, $A\omega^n$ is the dispersive component of the ionic conductivity of AC current. $'\omega'$ is the angular frequency, $'n'$ is the degree of freedom between the mobile ions and $'A'$ is a constant which indicates the strength of polarizability. It is observed in Fig. 13, for the concentration ratio of (10:01), (10:02), (10:5) [PVDF-HFP: (Mg $(ClO_4)_2$] polymer samples, the dc conductivity is independent of frequency and illustrated with a plateau for the long-range frequency. And for the concentration ratio of (10:03) & (10:04) [PVDF-HFP: (Mg $(ClO_4)_2$] polymer electrolytes, the ionic conductivity gradually increases with an increase of frequency since the dispersion of is more active ions and leads to segmental motion of ion from one site of polymer site to another site. It is attributed that at the high-frequency region, hopping of ions in forward-backward motion accomplishes a new atomic site which indeed helps in

the successful hoping of ions and for raising the ionic conductivity. The acquiring same initial site after forward-backward motion with respect to frequency is called unsuccessful hoping mechanism which is not noticed in the polymer sample [45]. Hence a successful hoping ion dispersion is seen in Fig. 13 for the composition ratio (10:03) & (10:04) [PVDF-HFP: (Mg $(ClO_4)_2$] polymer electrolytes. The back and forth hoping mechanism and translation motion are possible for these concentrations of samples, as their 'n' value reaches '1'. Another probability of quantum tunneling starts at the higher frequency region that leads to linear hoping of ions [46]. The results show the best ac ionic conductivity for the optimum concentration ratio of (10:04) [PVDF-HFP: (Mg $(ClO_4)_2$] polymer electrolytes. The calculated highest value of the real part of ac ionic conductivity is found to be $\sigma(\omega) = 0.00107\ Scm^{-1}$. Moreover, these results are very good and supporting for highest ionic conductivity and battery application of polymer electrolytes.

4. Conclusion

Poly (vinylidene-fluoride-hexafluoroproplyene) (PVDF-HFP) based polymer electrolyte membranes are prepared with the addition of different concentrations of $Mg(ClO_4)_2$ salt adapting solution casting process. The prepared polymer membranes were characterized by XRD, FTIR, SEM techniques. Electrochemical cell stability (cyclic voltammetry), dielectric spectroscopic and electrical properties are studied. SEM micrographs show the presence of interlinked micro-pores which promotes the mobility of Mg ions in the polymer electrolyte. The smooth morphological texture and uniform distribution of micro-pores confirm an increase in amorphous nature that attributes to enhance ionic conductivity. The XRD spectral peaks reveal a

reduction in the crystalline phase of the host polymer into amorphous. The spectroscopic FTIR vibrational bands show good complex formation between PVDF-HFP polymer and $Mg(ClO_4)_2$ salt. The prominent DC ionic conductivity of 7.7333×10^{-4} Scm^{-1} is obtained at room temperature. Mg / [PVDF-HFP: $Mg(ClO_4)_2$] / (I_2+C) solid polymer electrochemical cell is prepared and the discharge characteristics are investigated. The open-circuit voltage and short circuit current of the electrochemical cell is measured as 1.8V and 120 mA respectively. The electrochemical stability and reversibility of [Mg^{+2} / PVDF - HFP: $Mg(ClO_4)_2$ membrane /Carbon] cell is evaluated by cyclic voltammetry. The electrochemical stability with a constant voltage of 0.43volt in a positive cycle and 0.4 volts of negative potential is observed for the best compatibility of electrochemical membrane for battery applications. The dielectric spectroscopic studies of real (ε') & imaginary part of dielectric permittivity (ε'') are demonstrated by using Cole − cole plot. The measured values of static dielectric constant (ε_s), dynamic dielectric constant (ε_∞), dielectric strength ($\Delta\varepsilon$), dielectric loss (tanδ) reach maximum and but relaxation time (τ) decreases for an optimal concentration ratio of (100:40) PVDF-HFP: Mg (ClO_4)$_2$ polymer electrolyte that reveals fast hopping of ions in the polymer matrix from one site of the polymer chain to another. The frequency-dependent real part of complex ac conductivity of $0.00107\ Scm^{-1}$ is obtained at room temperature for [PVDF-HFP: $Mg(ClO_4)_2$] polymer-salt electrolyte.

References:

1. Alamgir, M., Abraham, K.M.., and G. Pistoia (Ed.).,(1994,)., Lithium batteries New Materials. Developments, Elsevier. vol. 5.p.93
2. Masayoshi Watanabe, Motoi Kanba, Hiroo Matsuda, Koichi Tsunemi, Katsuhiro Mizoguchi, EishunTsuchida,Isao Shinohara, Makromol. Chem., Rapid Commun. 2 (1981) 741
3. Gray, F.M., Vincent, C.A., Bruce, P.G., and Nowinski, J., B. Scrosati (Ed.), (1990) Second International Symposium on PolymerElectrolytes, Elsevier Applied Science, p. 299.
4. Abraham, K.M., Chowdari, B.V.R., et al. (Eds.), Solid State Ionic Materials and Applications, World Scientific Publishing Company, 1992, p. 277.
5. Yang, L. L. (1986). Ionic Conductivity in Complexes of Poly(ethylene oxide) and MgCl [sub2]. Journal of the Electrochemical Society, 133(7), 1380. doi:10.1149/1.2108891
6. Manjuladevi, R., Thamilselvan, M., Selvasekarapandian, S., Mangalam, R., Premalatha, M., and Monisha, S. (2017). Mg-ion conducting blend polymer electrolyte based on poly(vinyl alcohol)-poly (acrylonitrile) with magnesium perchlorate. Solid State Ionics, 308, 90–100. doi:10.1016/j.ssi.2017.06.002
7. Ponmani,S., Susithra, B., Ramesh and Prabhu, M., Conductivity and Dielectric behavior of PVdF-HFP/PEMA – Magnesium perchlorate solid polymer electrolyte Films for Mg-ion batteries. (April-2018). International Journal of Advance Engineering and Research Development (IJAERD). Volume 5, Special Issue 07.
8. Berthier,C., Gorecki, W., Minier,M., Armand,M.B., Chabagno, J.M. and Rigaud,P., (1983) Solid State Ionics, , 11, 91–95.
9. Jeong,S-K., Jo,Y-K., and Jo,N-J., (2006) ElectrochimicaActa, , 52, 1549–1555.
10. Shao, Y., Rajput, N. N., Hu, J., Hu, M., Liu, T., Wei, Z., Liu, J., (2015). Nanocomposite polymer electrolyte for rechargeable magnesium batteries. Nano Energy, 12, 750–759. doi:10.1016/j.nanoen.2014.12.028

11. Muldoon, J., Bucur, C. B., & Gregory, T. (2017). Fervent Hype behind Magnesium Batteries: An Open Call to Synthetic Chemists-Electrolytes and Cathodes Needed. AngewandteChemie International Edition, 56(40), 12064–12084. doi:10.1002/anie.201700673.
12. Bucur, C. B., Gregory, T., Oliver, A. G., & Muldoon, J. (2015). Confession of a Magnesium Battery. The Journal of Physical Chemistry Letters, 6(18), 3578–3591. doi:10.1021/acs.jpclett.5b01219
13. Ponmani, S., and Prabhu, M. R. (2018). Development and study of solid polymer electrolytes based on PVdF-HFP/PVAc: Mg (ClO4)2 for Mg ion batteries. Journal of Materials Science: Materials in Electronics, 29(17), 15086–15096.doi:10.1007/s10854-018-9649-0.
14. McGrath, L. M., Jones, J., Carey, E., and Rohan, J. F. (2019). Ionic Liquid Based Polymer Gel Electrolytes for Use with Germanium Thin Film Anodes in Lithium Ion Batteries. ChemistryOpen, 8(12), 1429– 1436. doi:10.1002/open.201900313.
15. Alamgir, M., and Abraham, K. M., in Lithium Batteries, New Materials,Developments and Perspectives, Vol. 5, G. Pistoia, Editor, Chap. 3, Elsevier, New York (1993). 5
16. Saikia, D., and Kumar, A. (2004). Ionic conduction in P(VDF-HFP)/PVDF–(PC + DEC)–$LiClO_4$ polymer gel electrolytes. ElectrochimicaActa, 49(16), 2581– 2589. doi:10.1016/j.electacta.2004.01.029
17. Sim, L. N., Majid, S. R., and Arof, A. K. (2012). FTIR studies of PEMA/PVdF-HFP blend polymer electrolyte system incorporated with LiCF3SO3 salt. Vibrational Spectroscopy, 58, 57–66. doi:10.1016/j.vibspec.2011.11.005
18. Du, C.-H., Zhu, B.-K., and Xu, Y.-Y. (2006). The effects of quenching on the phase structure of vinylidene fluoride segments in PVDF-HFP copolymer and PVDF-HFP/PMMA blends. Journal of Materials Science, 41(2), 417–421. doi:10.1007/s10853-005-2182-6
19. Salimi, A., and Yousefi, A. A. (2003). Analysis Method. Polymer Testing, 22(6), 699–704. doi:10.1016/s0142-9418(03)00003-5

20. Tian, X., and Jiang, X. (2008). Poly(vinylidene fluoride-co-hexafluoropropene) (PVDF-HFP) membranes for ethyl acetate removal from water. Journal of Hazardous Materials, 153(1-2), 128–135. doi:10.1016/j.jhazmat.2007.08.029
21. Luo, B., Wang, X., Wang, H., Cai, Z., and Li, L. (2017). P(VDF-HFP)/PMMA flexible composite films with enhanced energy storage density and efficiency. Composites Science and Technology, 151, 94–103. doi:10.1016/j.compscitech.2017.08.013
22. Prabakaran, K., Mohanty, S., and Nayak, S. K. (2015). Chemically exfoliated nanosilicate platelet hybridized polymer electrolytes for solid state dye sensitized solar cells. New Journal of Chemistry, 39(11), 8602–8613. doi:10.1039/c5nj00795j
23. Jiang, X., Zhao, X., Peng, G., Liu, W., Liu, K., and Zhan, Z. (2017). Investigation on crystalline structure and dielectric relaxation behaviors of hot pressed poly(vinylidene fluoride) film. Current Applied Physics, 17(1), 15–23. doi:10.1016/j.cap.2016.10.011
24. Gaur, M. S., Indolia, A. P., Rogachev, A. A., and Rahachou, A. V. (2015). Influence of SiO2 nanoparticles on morphological, thermal, and dielectric properties of PVDF. Journal of Thermal Analysis and Calorimetry, 122(3), 1403–1416. doi:10.1007/s10973-015-4872-x
25. Prabakaran, K., Mohanty, S., and Nayak, S. K. (2015). Improved electrochemical and photovoltaic performance of dye sensitized solar cells based on PEO/PVDF–HFP/silane modified TiO2 electrolytes and MWCNT/Nafion® counter electrode. RSC Advances, 5(51), 0491–40504. doi:10.1039/c5ra01770j
26. Ramesh, S., and Lu, S.-C. (2011). Effect of lithium salt concentration on crystallinity of poly(vinylidene fluoride-co-hexafluoropropylene)-based solid polymer electrolytes. Journal of Molecular Structure, 994(1-3), 403–409. doi:10.1016/j.molstruc.2011.03.065
27. Prabakaran, K., Palai, A. K., Mohanty, S., and Nayak, S. K. (2015). Aligned carbon nanotube/polymer hybrid electrolytes for high performance dye

sensitized solar cell applications. RSC Advances, 5(82), 66563–66574. doi:10.1039/c5ra10843h

28. Perumal, P., Abhilash, K. P., P.Sivaraj, and Selvin, P. C. (2019). Study on Mg-ion conducting solid biopolymer electrolytes based on tamarind seed polysaccharide for magnesium ion batteries. Materials Research Bulletin. doi:10.1016/j.materresbull.2019.05.015
29. Ataollahi, N., Ahmad, A., Hamzah, H., Rahman, M.Y.A., and Mohamed, N.S., Preparation and Characterization of PVDF-HFP/MG49 Based Polymer Blend Electrolyte; Int. J. Electrochem. Sci., 7 (2012) 6693 – 6703
30. Bormashenko, Y., Pogreb, R., Stanevsky, O., and Bormashenko, E. (2004). Vibrational spectrum of PVDF and its interpretation. Polymer Testing, 23(7), 791–796. doi:10.1016/j.polymertesting.2004.04.001
31. Lanceros-Méndez, S., Mano, J. F., Costa, A. M., and Schmidt, V. H. (2001). FTIR and DSC studies of mechanically deformed β-pvdf films. Journal of Macromolecular Science, Part B, 40(3-4), 517–527. doi:10.1081/mb-100106174
32. Nallaswamy, P., and Mohan, S., Vibrational spectroscopic characterization of from II poly(Vinylidene fluoride), Indian Journal of Pure & Applied Physics Vol. 43, November 2005, pp.821-827.
33. TianKhoon, L., Ataollahi, N., Hassan, N. H., and Ahmad, A. (2015). Studies of porous solid polymeric electrolytes based on poly (vinylidene fluoride) and poly (methyl methacrylate) grafted natural rubber for applications in electrochemical devices. Journal of Solid State electrochemistry, 20(1), 203–213. doi:10.1007/s10008-015-3017-2
34. Tafur, J., Santos, F., and Romero, A. (2015). Influence of the Ionic Liquid Type on the Gel Polymer Electrolytes Properties. Membranes, 5(4), 752–771. doi:10.3390/membranes5040752
35. Van der Marel, H. W., and Krohmer, P. (1969). O-H stretching vibrations in Kaolinite and related minerals. Contributions to Mineralogy and Petrology, 22(1), 73–82. doi:10.1007/bf00388013

36. Sharma, J., and Hashmi, S. (2018). Magnesium ion-conducting gel polymer electrolyte nanocomposites: Effect of active and passive nanofillers. Polymer Composites. doi:10.1002/pc.24853
37. Gohel, K., and Kanchan, D. K. (2018). Ionic conductivity and relaxation studies in PVDF-HFP:PMMA-based gel polymer blend electrolyte with LiClO4 salt. Journal of Advanced Dielectrics, 08(01), 850005.doi:10.1142/s2010135x18500054.
38. Wagner J.B. and Wagner C., J. Chem. Phys., (1957) Vol.26, 1957.
39. Jaipal Reddy, M., Sreekanth, T., &SubbaRao, U. V., (1999). Study of the plasticizer effect on a (PEO+NaYF4) polymer electrolyte and its use in an electrochemical cell. Solid State Ionics, 126(1-2), 55–63. doi:10.1016/s0167-2738(99)00225-8.
40. Atyia, H.E.; Hegab, N.A. (2016). *Dielectric relaxation behavior and conduction mechanism of Te46As32Ge10Si12 films.. Optik - International Journal for Light and Electron Optics, 127(15), 6232–6242.* doi:10.1016/j.ijleo.2016.04.024
41. Cole, Kenneth S.; Cole, Robert H. (1941). *Dispersion and Absorption in Dielectrics I. Alternating Current Characteristics. , 9(4), 341–0.* doi:10.1063/1.1750906.
42. Kenneth S. Robert H. Cole J. Chem. Phys. **9**, 341 (1941); https://doi.org/10.1063/1.1750906.
43. Arya, A., & Sharma, A. L. (2018). *Effect of salt concentration on dielectric properties of Li-ion conducting blend polymer electrolytes. Journal of Materials Science: Materials in Electronics.* doi:10.1007/s10854-018-9905-3
44. Hadi, Jihad M.; Aziz, Shujahadeen B.; Mustafa, Muhammed Salih; Hamsan, Muhamad H.; Abdulwahid, Rebar T.; Kadir, Mohd F.Z.; Ghareeb, Hewa Osman (2020). *Role of nano-capacitor on dielectric constant enhancement in PEO:NH4SCN:xCeO2 polymer nano-composites: Electrical and electrochemical properties. Journal of Materials Research and Technology, 9(4), 9283–9294.* doi:10.1016/j.jmrt.2020.06.022
45. Dhahri, Ah; Dhahri, E.; Hlil, E. K. (2018). *Electrical conductivity and dielectric behaviour of nanocrystalline $La_{0.6,}$ $Gd_{0.1}$ $Sr_{0.3}$ $Mn_{0.75}$ $Si_{0.25}$ O_3. RSC Advances, 8(17), 9103–9111.* doi:10.1039/c8ra00037a
46. B. Aziz, Shujahadeen (2018). *Electrical and Dielectric Properties of Copper Ion Conducting Solid Polymer Electrolytes Based on Chitosan: CBH Model for Ion Transport Mechanism. International Journal of Electrochemical Science, (), 3812–3826.* doi:10.20964/2018.04.10

Figures

Figure 1

Illustrates a picture of prepared (PVDF-HFP: Mg (ClO4)2) polymer-salt electrolyte Membrane.

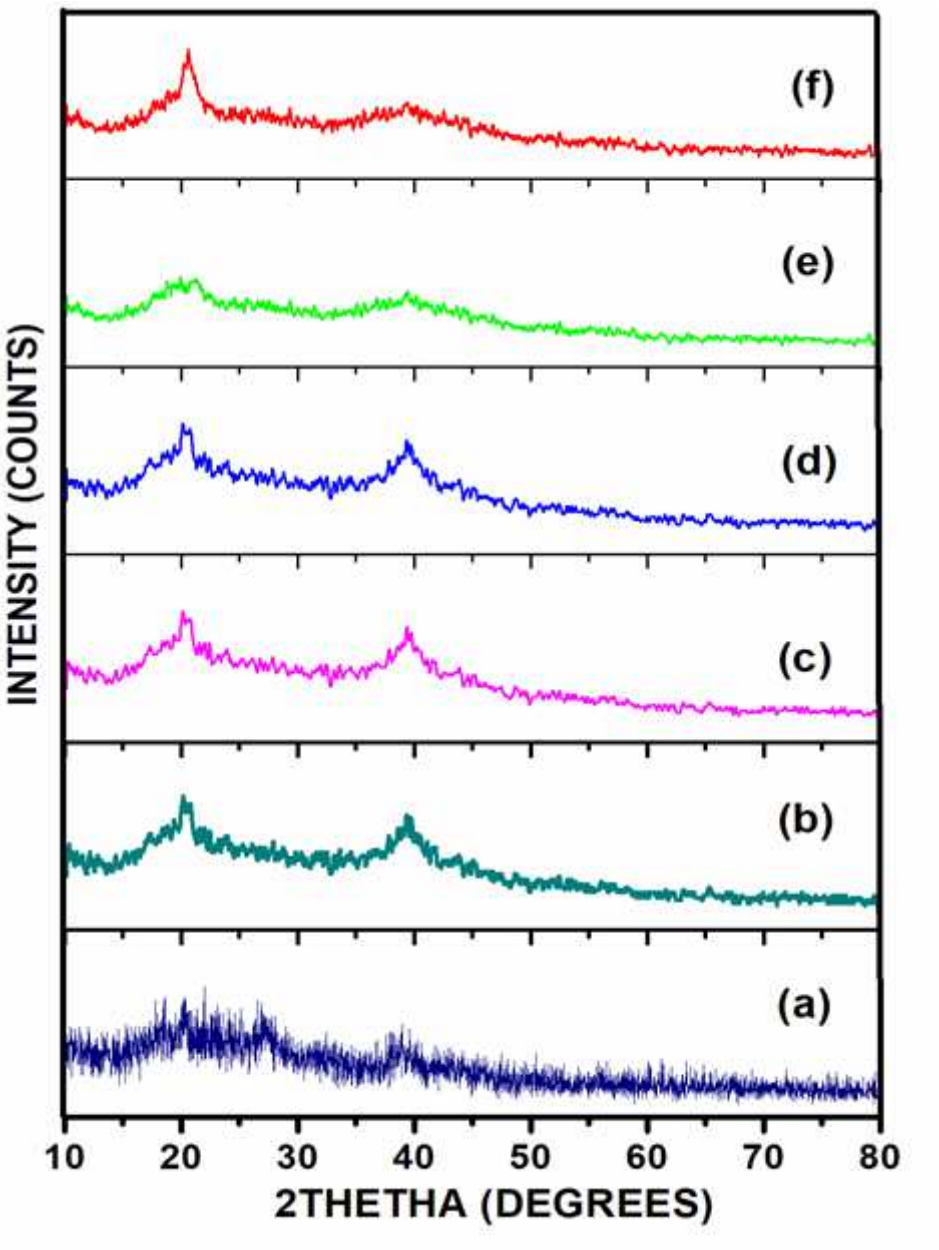

Figure 2

Illustrates XRD spectrum of PVDF-HFP polymer with different concentrations of Mg(ClO4)2 salt (a) 0% (b) 10% (c) 20% (d) 30% (e) 40% and (f) 50%

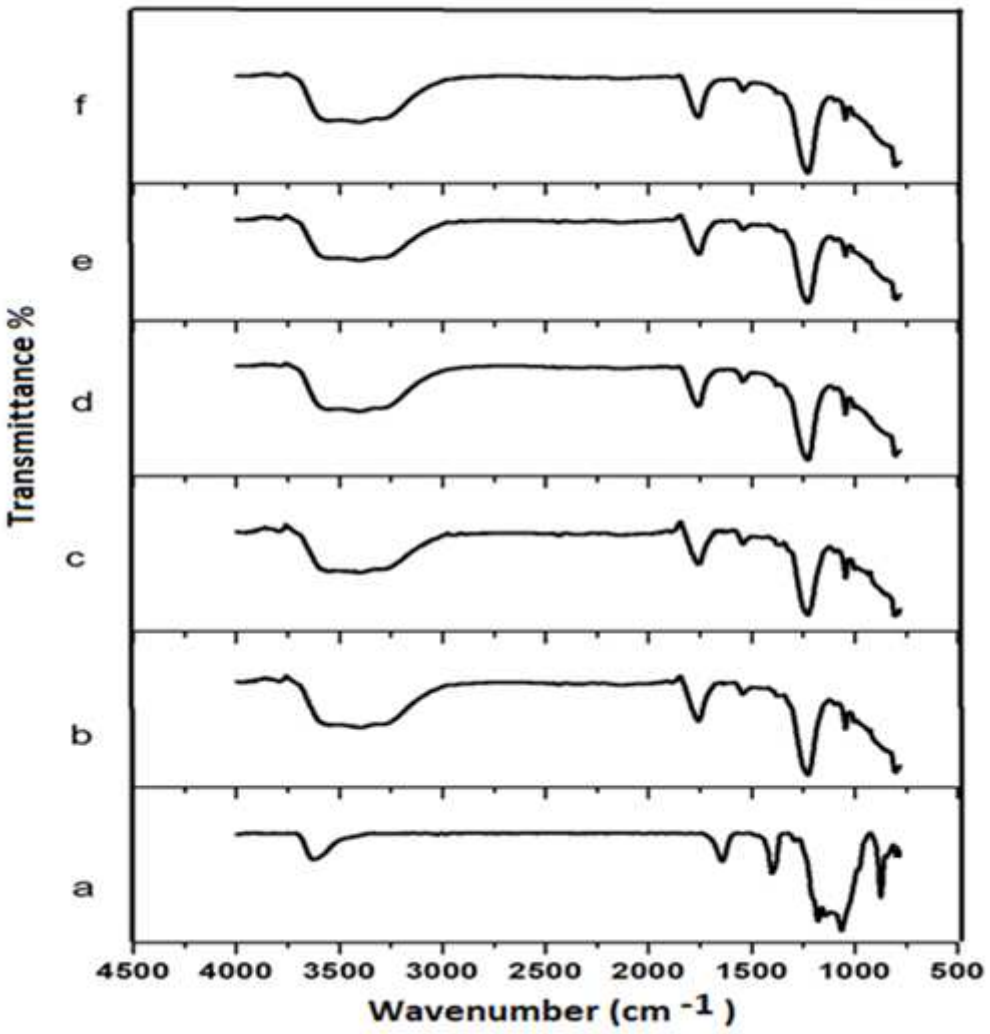

Figure 3

FTIR spectrum of PVDF-HFP polymer blend with different concentrations of Mg(ClO4)2 salt (a) 0% (b) 10% (c) 20% (d) 30% (e) 40% and (f) 50%

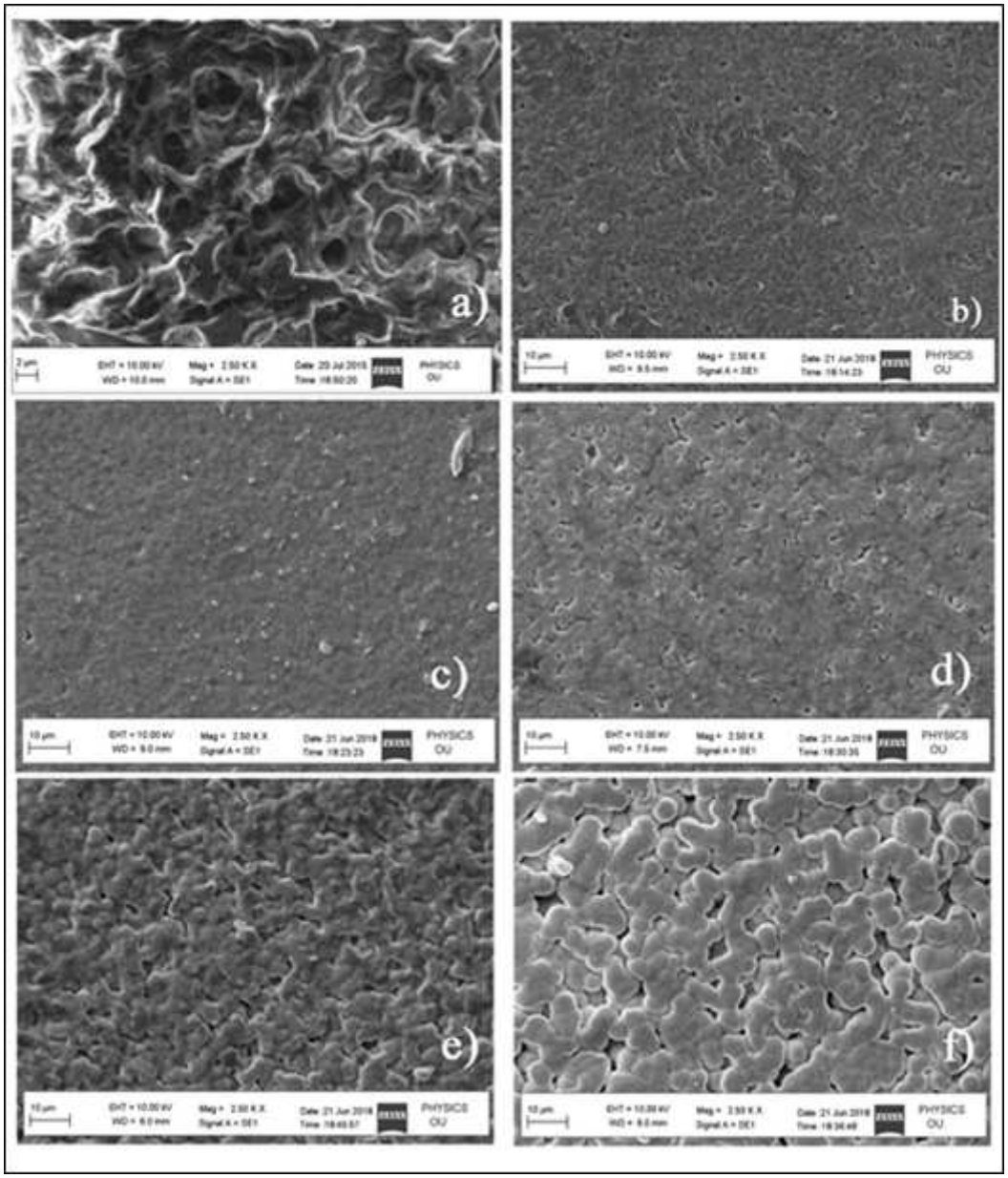

Figure 4

Illustrates SEM micrographs of of PVDF-HFP polymer with different concentration of Mg (ClO4)2 salt (a) 0% (b) 10% (c) 20% (d) 30% (e) 40% and (f) 50%

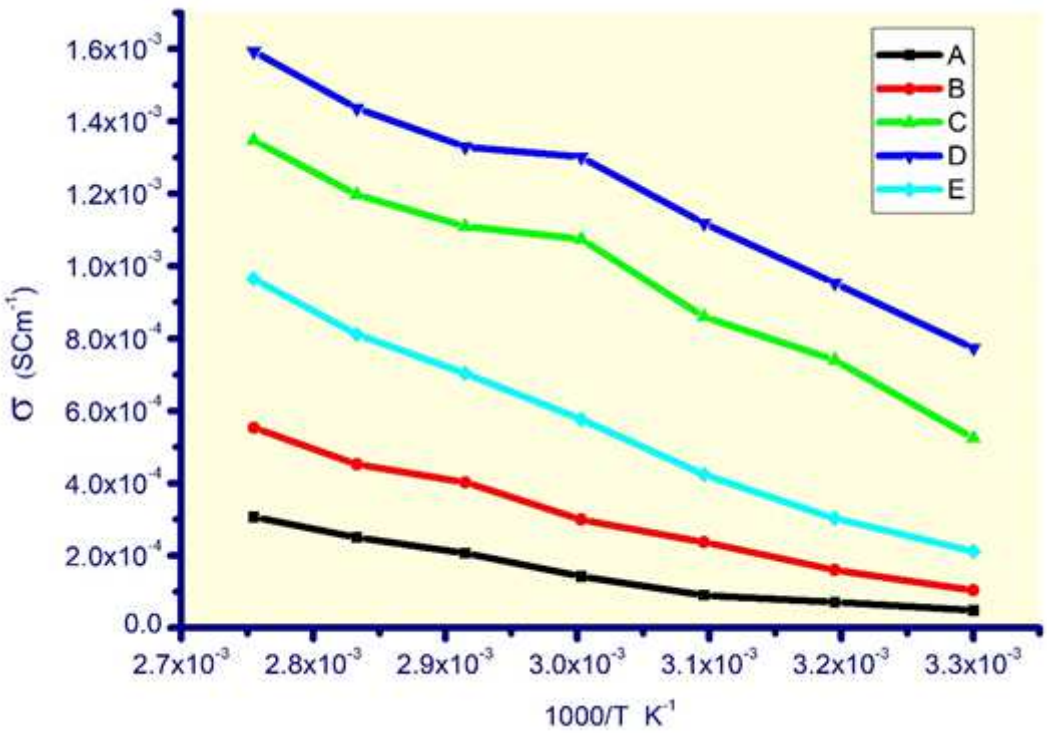

Figure 5

Temperature dependent DC conductivity of PVDF-HFP with various concentration of Mg (ClO4)2 polymer-salt electrolytes (A) 10% (B) 20% (C) 30% (D) 40% and (E) 50%

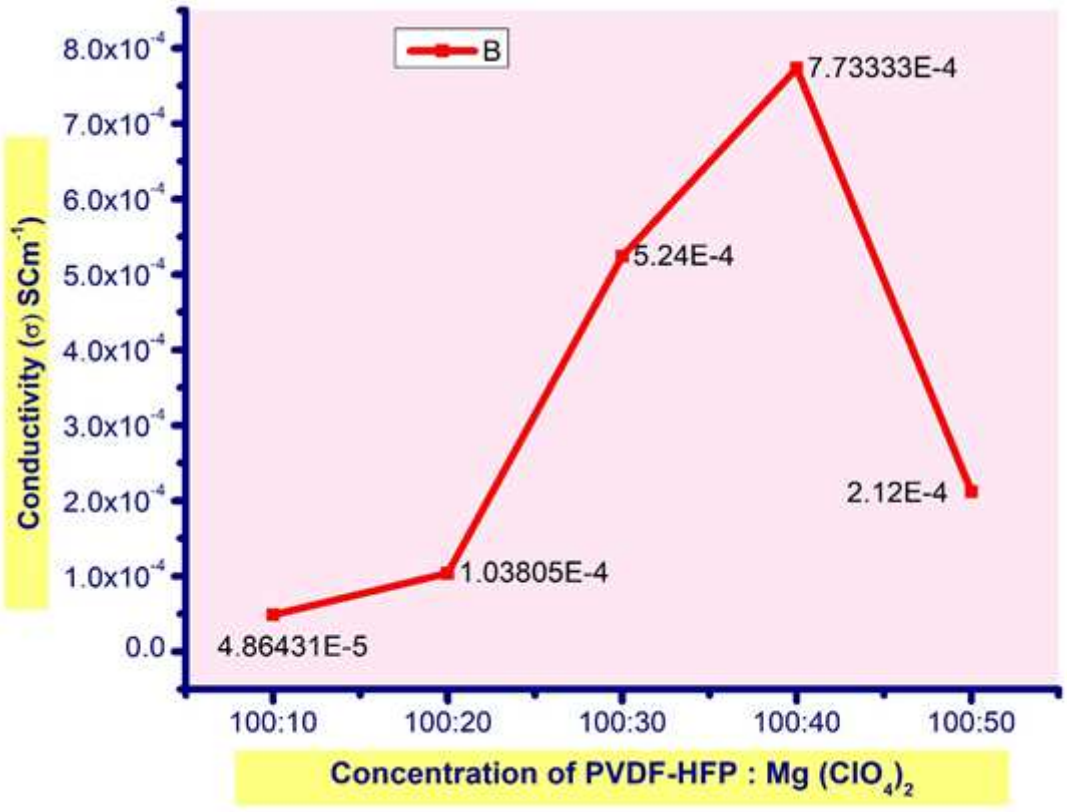

Figure 6

Variation of DC conductivity for different concentrations of Mg (ClO4)2 salt in PVDF-HFP polymer

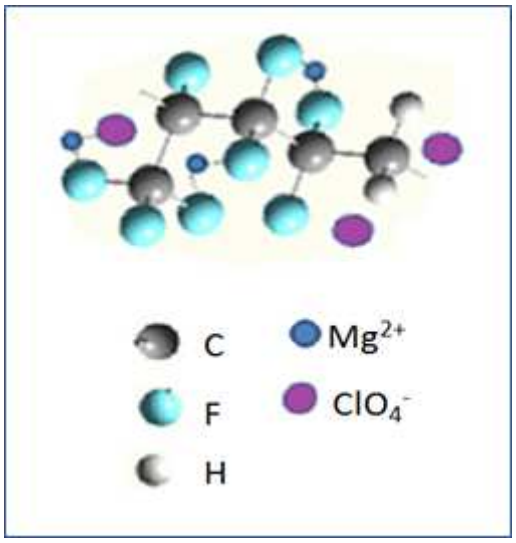

Figure 7

Structural Model of PVDF-HFP: Mg (ClO4)2 Solid Polymer electrolyte membrane

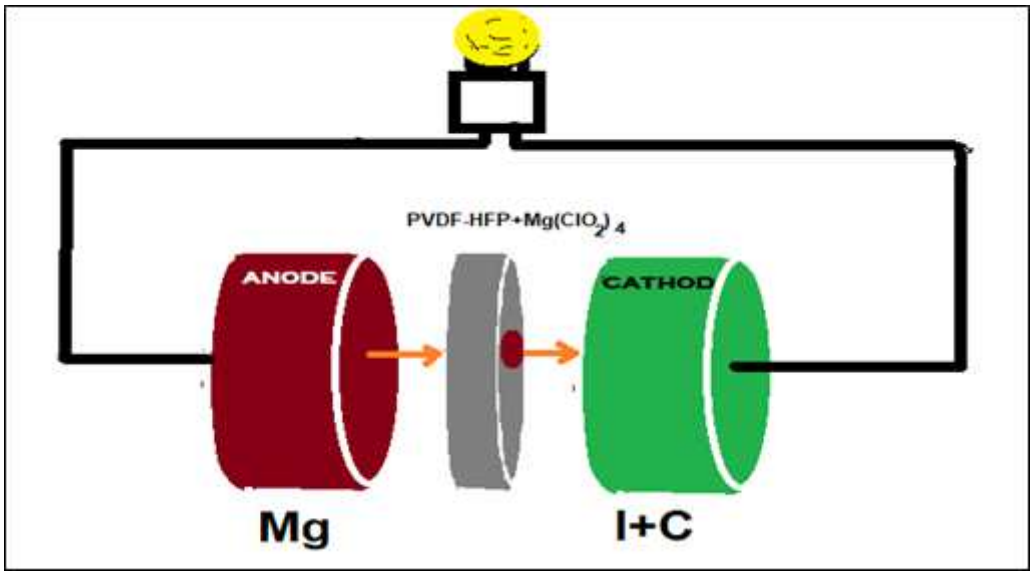

Figure 8

Mg2+ ion electrochemical cell of Mg / [PVDF-HFP: Mg(ClO4)2] (100:40) / I2+C for the polymer electrolyte

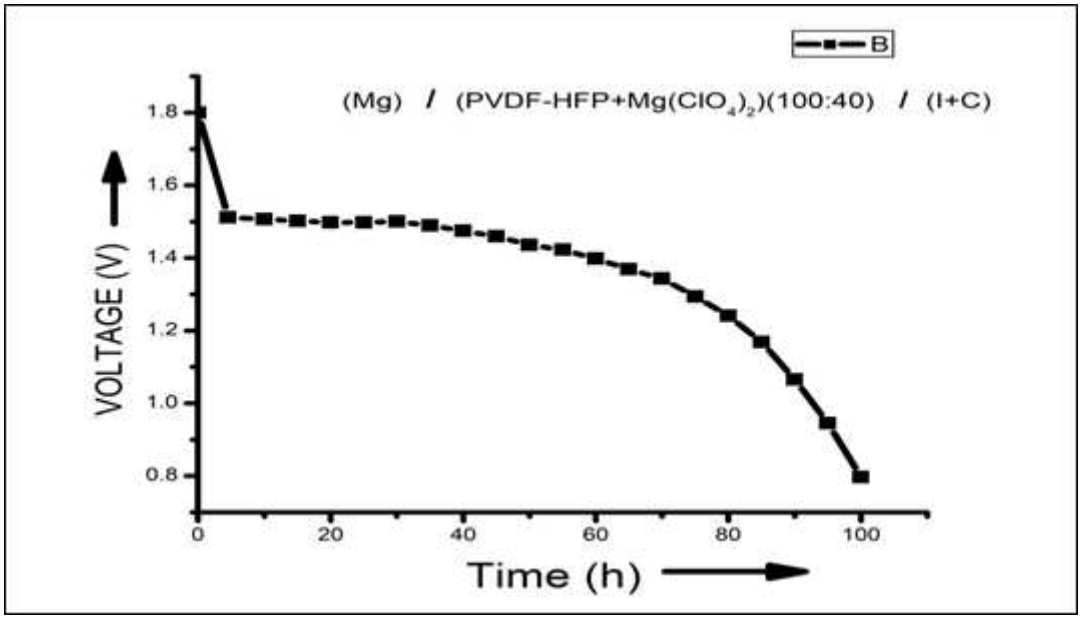

Figure 9

Voltage Vs Time curve illustrates discharge characteristics of an Electrochemical cell of Mg/100 PVDF-HFP: 40 Mg(ClO4)2 / I2 +C

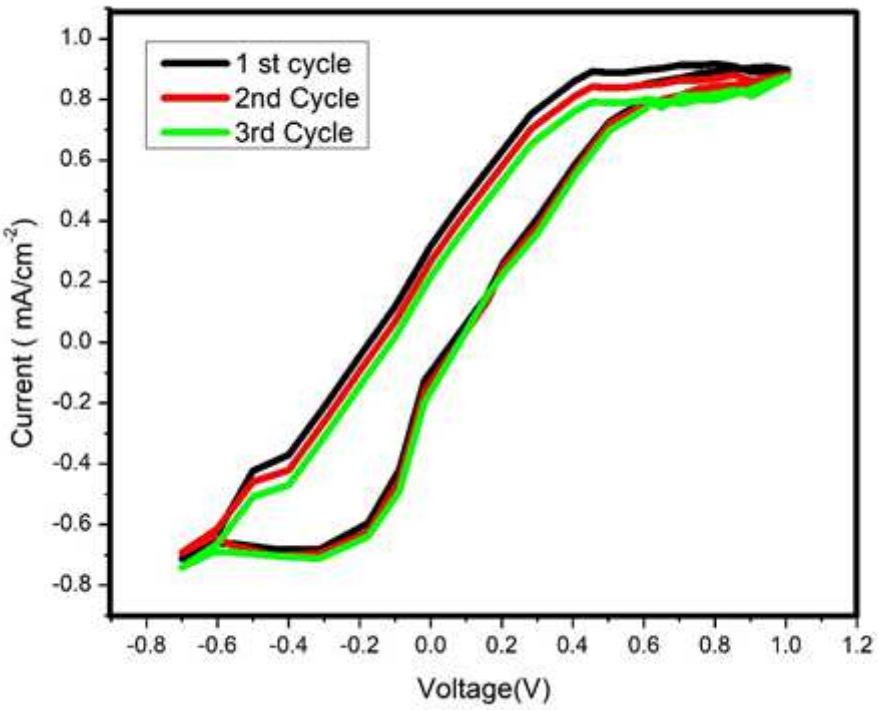

Figure 10

Cyclic voltammetry (CV) curves of PVDF-HFP: Mg (ClO4)2 polymer electrolyte films at a time interval of 24 hours.

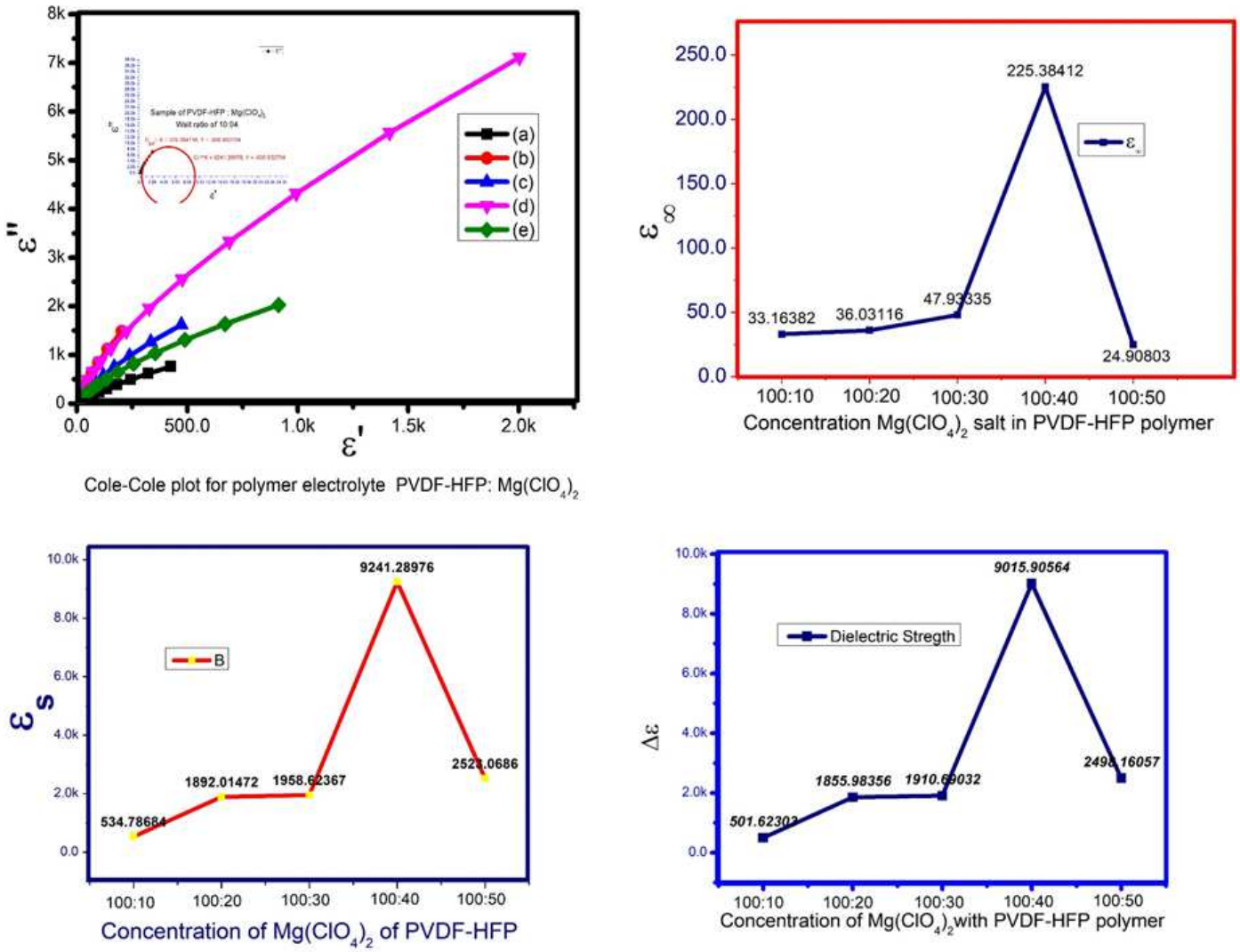

Figure 11

a) Variation of ε^" imaginary dielectric constant against ε^' in the Mg (ClO4)2 based solid PVDF-HFP polymer electrolyte b) Variation of dynamic dielectric constant (□_∞) with the concentration of Mg (ClO4)2 salt in the PVDF-HFP polymer electrolyte c) Variation of static dielectric constant with the concentration of Mg (ClO4)2 salt in the PVDF-HFP polymer electrolyte d) Variation of dielectric strength (□□) with the concentration of Mg (ClO4)2 salt in the PVDF-HFP polymer electrolyte

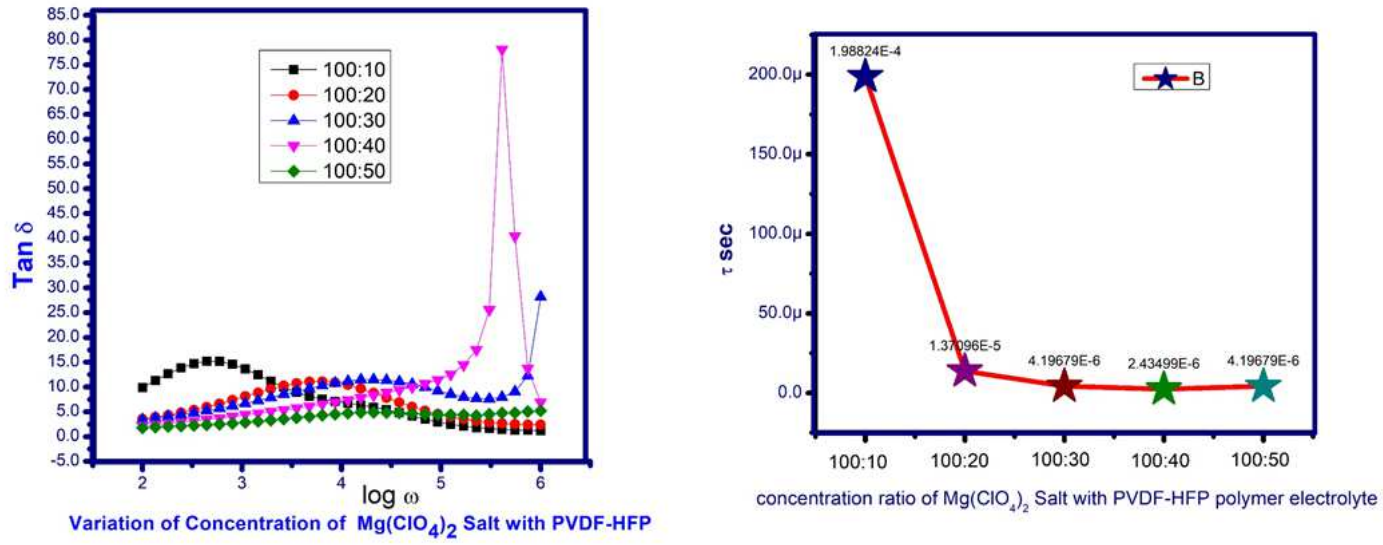

Figure 12

a) Variation of dielectric loss (Tanδ) against logω of Mg(ClO4)2 in the PVDF-HFP polymer electrolyte. b) Variation of relaxation time against concentration of Mg(ClO4)2 salt with PVDF-HFP solid polymer electrolyte.

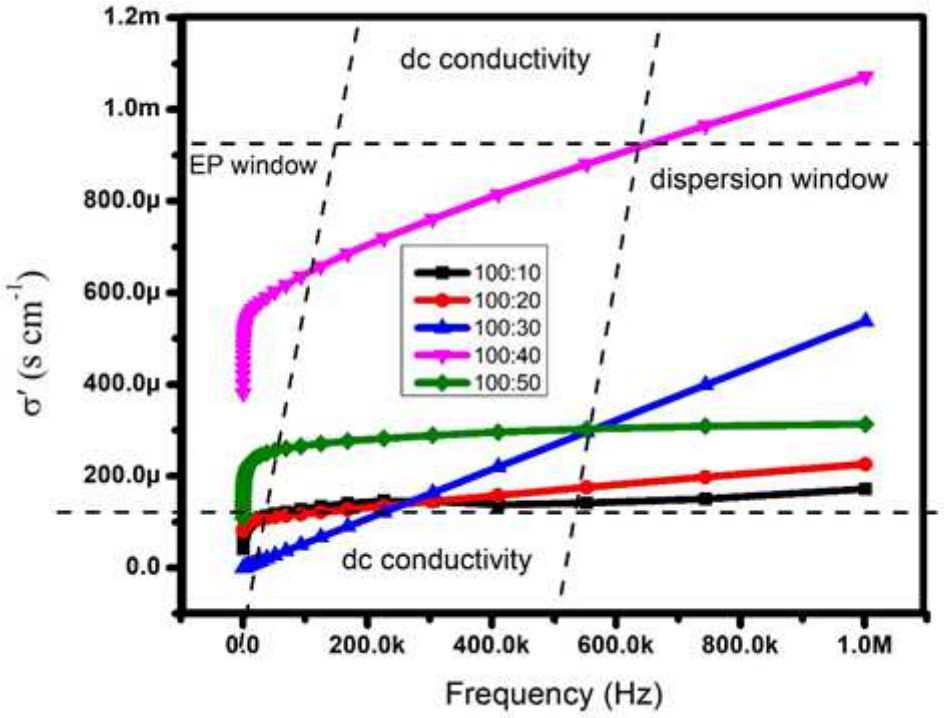

Figure 13

Variation of real part of conductivity against frequency for different concentration of Mg(ClO4)2 salt in PVDF-HFP solid polymer electrolyte